



## Cyclohexane 1,3-diones and their inhibition of mutant SOD1-dependent protein aggregation and toxicity in PC12 cells

Wei Zhang<sup>a,†</sup>, Radhia Benmohamed<sup>b</sup>, Anthony C. Arvanites<sup>b,‡</sup>, Richard I. Morimoto<sup>c</sup>, Robert J. Ferrante<sup>d,e</sup>, Donald R. Kirsch<sup>b</sup>, Richard B. Silverman<sup>a,f,\*</sup>

<sup>a</sup> Department of Chemistry, Northwestern University, Evanston, IL 60208-3113, USA

<sup>b</sup> Cambria Pharmaceuticals, Cambridge, MA 02142, USA

<sup>c</sup> Department of Molecular Biosciences, Rice Institute for Biomedical Research, Northwestern University, Evanston, IL 60208-3500, USA

<sup>d</sup> Neurological Surgery, Neurology, and Neurobiology Departments, University of Pittsburgh, Pittsburgh, PA 15213, USA

<sup>e</sup> The Geriatric Research Educational and Clinical Center (00-GR-H), V.A. Pittsburgh Healthcare System, 7180 Highland Drive, Pittsburgh, PA 15206, USA

<sup>f</sup> Department of Molecular Biosciences, Chemistry of Life Processes Institute, Center for Molecular Innovation and Drug Discovery, Northwestern University, Evanston, IL 60208-3113, USA

### ARTICLE INFO

#### Article history:

Received 22 September 2011

Revised 15 November 2011

Accepted 19 November 2011

Available online 30 November 2011

#### Keywords:

Cyclohexane-1,3-dione

Amyotrophic lateral sclerosis

Mutant G93A SOD1

Blood–brain barrier penetration

### ABSTRACT

Amyotrophic lateral sclerosis (ALS) is a fatal neurodegenerative disease characterized by the progressive loss of motor neurons. Currently, there is only one FDA-approved treatment for ALS (riluzole), and that drug only extends life, on average, by 2–3 months. Mutations in Cu/Zn superoxide dismutase (SOD1) are found in familial forms of the disease and have played an important role in the study of ALS pathophysiology. On the basis of their activity in a PC12-G93A-YFP high-throughput screening assay, several bioactive compounds have been identified and classified as cyclohexane-1,3-dione (CHD) derivatives. A concise and efficient synthetic route has been developed to provide diverse CHD analogs. The structural modification of the CHD scaffold led to the discovery of a more potent analog (**26**) with an EC<sub>50</sub> of 700 nM having good pharmacokinetic properties, such as high solubility, low human and mouse metabolic potential, and relatively good plasma stability. It was also found to efficiently penetrate the blood–brain barrier. However, compound **26** did not exhibit any significant life span extension in the ALS mouse model. It was found that, although **26** was active in PC12 cells, it had poor activity in other cell types, including primary cortical neurons, indicating that it can penetrate into the brain, but is not active in neuronal cells, potentially due to poor selective cell penetration. Further structural modification of the CHD scaffold was aimed at improving global cell activity as well as maintaining potency. Two new analogs (**71** and **73**) were synthesized, which had significantly enhanced cortical neuronal cell permeability, as well as similar potency to that of **26** in the PC12-G93A assay. These CHD analogs are being investigated further as novel therapeutic candidates for ALS.

© 2011 Elsevier Ltd. All rights reserved.

### 1. Introduction

Amyotrophic lateral sclerosis (ALS), an orphan neurodegenerative disease, is defined by the progressive loss of motor neurons. There are an estimated 87,000 ALS patients worldwide, who survive, on average, only 2–5 years after diagnosis.<sup>1,2</sup> Riluzole is the only FDA approved drug for the treatment of ALS; however, it only extends life by 2–3 months.<sup>1</sup> Although only 5–10% of ALS cases are

familial, similar clinical and pathological features are exhibited in familial and sporadic forms of the disease. Mutations in Cu/Zn superoxide dismutase (SOD1), which cause misfolding and aggregation of the protein, are responsible for the disease in a subgroup of patients with familial ALS.<sup>1,2</sup> The cultured cell model, PC12-G93A-YFP, developed by Matsumoto and co-workers,<sup>3</sup> was utilized to develop a high-throughput screen (HTS) as a cellular model of ALS, which identified active compounds in the cytotoxicity protection assay.<sup>4</sup> In this assay, G93A SOD1 aggregation is cytotoxic and inhibition of SOD1 mutant protein aggregation is cytoprotective. The percentage of cell survival is determined from the maximum cell viability after exposure of test compounds and EC<sub>50</sub> values are determined from the decrease in the cytotoxicity of mutant SOD1-G93A-YFP aggregation by the treatment with test compounds. Three chemotypes were identified in this high-throughput screen: arylsulfanyl pyrazolones,<sup>5</sup> pyrimidine 2,4,6-triones,<sup>6</sup> and

\* Corresponding author. Tel.: +1 847 491 5663; fax: +1 847 491 7713.

E-mail address: [Agman@chem.northwestern.edu](mailto:Agman@chem.northwestern.edu) (R.B. Silverman).

† Present address: State Key Laboratory of Organometallic Chemistry, Shanghai Institute of Organic Chemistry, Chinese Academy of Sciences, No. 345, Lingling Road, Shanghai 230032, China.

‡ Present address: Harvard Stem Cell Institute, Harvard University, Cambridge, MA 02138, USA.

cyclohexane 1,3-diones (CHDs). They all showed 100% efficacy (cell viability) compared with the positive control (radicol, 85% efficacy) in the cytotoxicity assay. EC<sub>50</sub> values of the most potent CHDs ranged between 3 μM and 8 μM in the protection assay. Here, we describe the SAR and pharmacokinetic studies of this class of compounds as inhibitors of protein aggregation caused by mutant SOD1.

## 2. Results and discussion

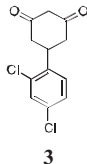
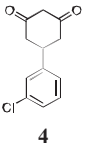
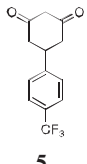
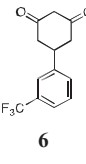
A concise and efficient synthetic route to CHD analogs is summarized in Scheme 1.<sup>7</sup> This two-step procedure made it possible to apply parallel synthesis methods. Commercially available or previously synthesized aldehydes (**1**) were used as starting materials, which were conveniently converted to intermediates **2** in high yields. CHDs were then obtained in one pot in satisfactory yields and purity by treatment with diethyl malonate followed by hydrolysis and decarboxylation. More than 120 analogs were obtained by this simple protocol.

On the basis of their activity in the PC12-G93A-YFP high-throughput screening assay,<sup>4</sup> several active CHD analogs were identified (Table 1). In this assay, G93A mutant SOD1 protein aggregates are observed following treatment with the proteasome inhibitor MG132. The formation of these SOD1 aggregates is cytotoxic in this model. Therefore, cell survival is measured to determine test compound efficacy. Active CHD analogs showed 100% efficacy (cell viability) compared with the positive control radicol (85% efficacy). EC<sub>50</sub> values of the most potent compounds ranged between 3 and 8 μM in the protection assay.

Various aromatic aldehydes were used to synthesize CHD analogs, as all of the active CHD analogs contained a phenyl or substituted phenyl group. Size, electronic properties, and positional effects were tested by modifying the substituents on the aromatic ring. Several conclusions can be drawn regarding a structure–activity relationship (Table 2): (1) electronic properties of the substituted groups do not affect the activity of analogs; (2) the *meta* position is much more important than the other positions; (3) the size of the *meta*-substituents is very crucial; and (4) CF<sub>3</sub> is a favored substituent to increase the potency. Finally, it was found that the 3,5-CF<sub>3</sub> substituted analog (**26**, Table 2) had superior potency relative to the other analogs.

Pharmacokinetic studies with **26** showed that it had good solubility (≥500 μM), high human and mouse (both T<sub>1/2</sub> ≥ 180 min) microsomal stability, and an oral bioavailability of 89% (Table 3a and b). Caco-2 permeability (A→B, 38 cm<sup>-6</sup>/s) indicated promising ability for good absorption, and a relatively low flux in the B→A direction (5.7 cm<sup>-6</sup>/s), giving a low efflux ratio (B→A/A→B, 0.2). A maximum tolerated dose for **26** of 80 mg/kg was determined by intraperitoneal injection in mice starting at 5 mg/kg and doubling the compound b.i.d. each day, once in the morning and once mid afternoon. Plasma concentration and blood brain barrier penetration of **26** were determined in G93A SOD1 transgenic mice. Compound **26** produces stable plasma concentrations between 3 and 12 h and brain concentration was, therefore, determined at

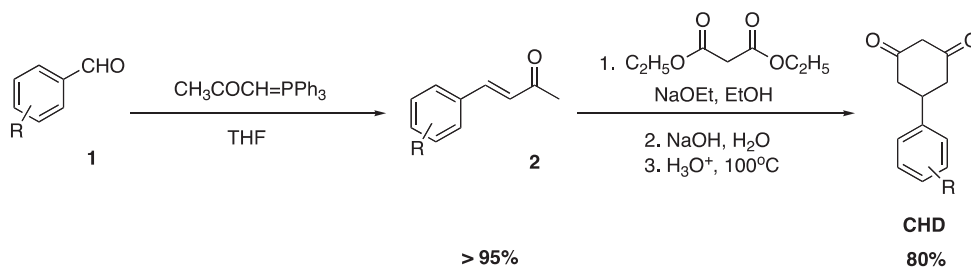
**Table 1**  
Selected examples from the preliminary HTS results<sup>4</sup>

CHD	EC <sub>50</sub> <sup>a</sup> (μM)	CHD	EC <sub>50</sub> (μM)
	4.57		6.52
	8.30		3.33

<sup>a</sup> An analog was considered to be inactive when EC<sub>50</sub> >32 μM.

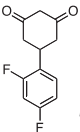
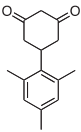
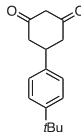
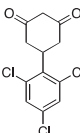
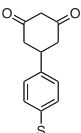
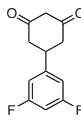
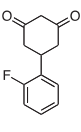
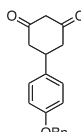
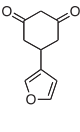
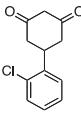
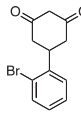
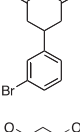
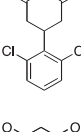
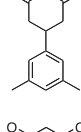
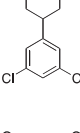
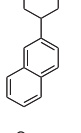
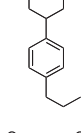
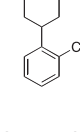
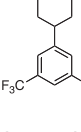
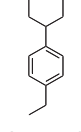
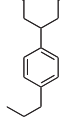
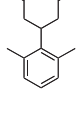
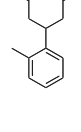
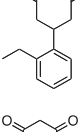
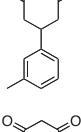
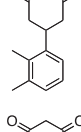
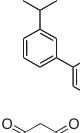
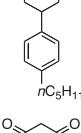
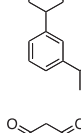
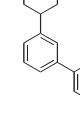
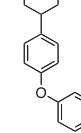
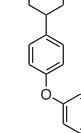
4 h, within the concentration plateau. At this time point the brain concentration was determined to be 579 μM and plasma concentration 675 μM, producing a very good brain–plasma ratio (B/P) of 0.86. Compound **26** (10 μM) was subjected to the LeadProfiling-Screen of MDS Pharma Services, a panel of 68 radioligand receptor assays, and none was positive (all exhibited <20% [mostly <10%] inhibition). At 10 μM concentration, **26** inhibited the hERG channel by only 7.8%, indicating a low probability of it leading to arrhythmias in humans.

Consequently, **26** was selected for testing in the ALS mouse model.<sup>8</sup> Compound **26** demonstrated no significant activity in the mutant SOD1 G93A transgenic mice (Fig. 1). At the highest dose (20 mg/kg) there was a non-significant 4.6% increase in survival. We did not, however, use a dose that resulted in adverse events or worsening survival, as compared to the untreated G93A mice and, as such, the greatest optimal dose might not have been achieved. Given the good potency, aqueous solubility, stability to microsomes, high oral bioavailability, blood–brain barrier penetration, and volume of distribution (V<sub>ss</sub>), the in vivo inactivity was surprising. One parameter that was different from that seen for other compounds in our research program that were active in G93A SOD1 ALS mice, was the smaller volume of distribution, which was only ~15–25% that of active compounds. We, therefore, became concerned that the lack of efficacy might be the result of the inability of **26** to penetrate into certain cells, particularly neurons. To address this concern, a qualitative primary cortical neuron assay was developed. As described in the experimental section, this assay is not based on the ability of the compounds to reduce mutant SOD1 aggregation, but rather on a related activity (protection against MG132 toxicity), which made it possible to conveniently test compounds on a wide variety of cell types. While the assay measures activity and not cell penetration per se, it nevertheless allowed us to determine whether compounds were active in the target nerve cells and, if necessary, to guide analog synthesis for identification of compounds with the desired activity. As can be



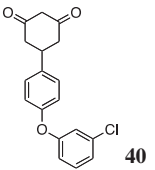
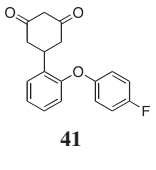
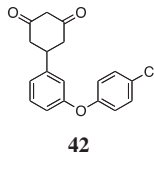
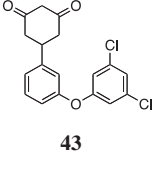
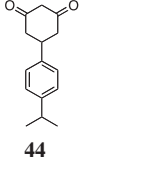
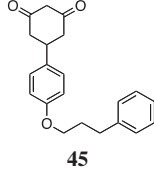
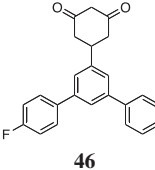
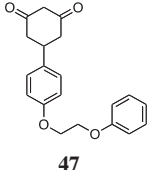
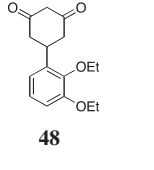
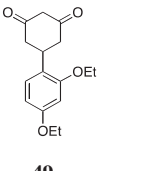
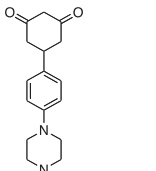
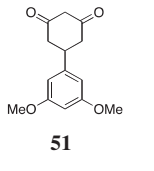
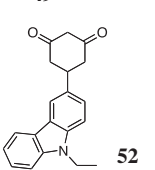
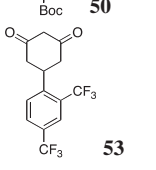
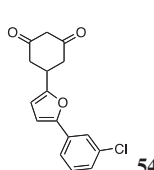
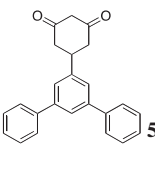
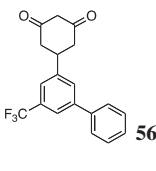
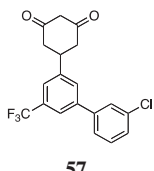
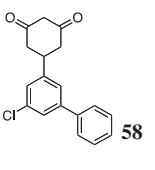
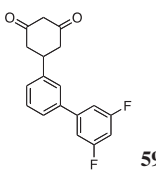
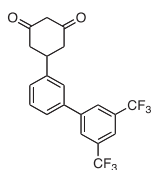
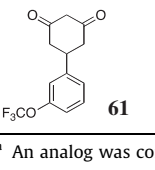
**Scheme 1.** General synthetic route to cyclohexane 1,3-dione (CHD) analogs.

**Table 2**  
Selected examples of synthetic CHD analogs in the PC12-G93A-YFP cell-based assay

CHD	EC <sub>50</sub> <sup>a</sup> (μM)	CHD	EC <sub>50</sub> (μM)	CHD	EC <sub>50</sub> (μM)
	>32		>32		9.93
	7.01		>32		8.20
	>32		>32		>32
	>32		>32		>32
	28.7		24.3		2.40
	2.35		6.21		2.71
	3.20		0.70		2.22
	2.22		2.70		3.39
	3.16		4.81		2.39
	1.23		2.01		1.58
	3.51		2.37		2.88

(continued on next page)

Table 2 (continued)

CHD	EC <sub>50</sub> <sup>a</sup> (μM)	CHD	EC <sub>50</sub> (μM)	CHD	EC <sub>50</sub> (μM)
	3.60		1.16		2.18
	6.66		4.09		1.30
	3.07		1.56		3.99
	1.49		8.29		5.20
	3.09		2.56		2.71
	2.53		0.73		1.56
	1.10		1.24		2.15
	2.04				

<sup>a</sup> An analog was considered to be inactive when EC<sub>50</sub> >32 μM.

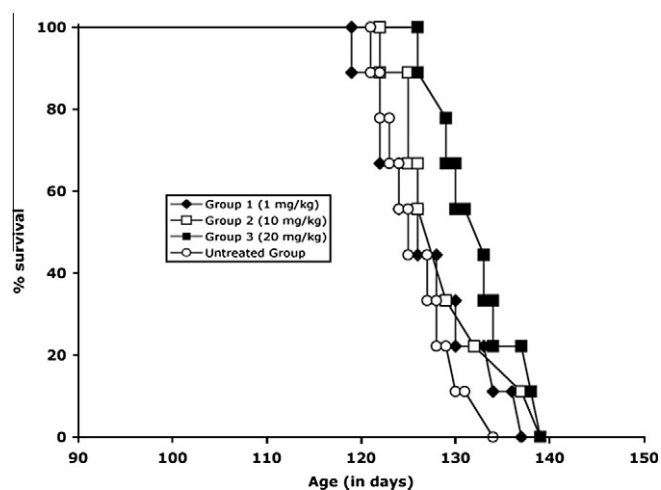
seen in Table 4, although **26** is active in PC12 cells, which was the cell line used in the high-throughput screen of compounds, it is inactive in a variety of other cell types, including neuronal cells. Whether this is due to cell penetration or other factors remains an open question. However, lack of activity on the target cell type, neurons, provides a plausible explanation for lack of activity in the ALS mouse model. Further modification of CHD analogs was aimed at improving their neuronal cell activity as well as maintaining their potency. To that end, different linkages between the cyclohexane 1,3-dione core and the substituted phenyl group were synthesized and tested. This would change the geometry of the

molecule as well as make it more flexible, which might have an effect on cell permeability (Fig. 2).

The synthetic route to the CHD analogs shown in Scheme 1, also was applicable to the synthesis of the modified scaffolds in Figure 1. The R groups selected were 3-Cl, 3-CF<sub>3</sub>, 3,5-Cl, or 3,5-CF<sub>3</sub>, because previous analogs with these groups were among the most potent analogs. On the basis of PC12-G93A-YFP high-throughput screening assay,<sup>4</sup> activities of some of the new CHD analogs were measured (Table 5). All of these analogs were also screened in the primary cortical neuron assay. Only two CHD scaffolds (**71** and **73**) showed consistently positive results in all cell lines,

**Table 3**(A) Intravenous pharmacokinetics of **26** (1 mg/kg) in Sprague-Dawley rat; (B) oral pharmacokinetics of **26** (1 mg/kg) in Sprague-Dawley rat

(A)					
AUC <sup>a</sup> last (ng h/mL)	AUC/dose (ng h/mL/dose)	Cl (mL/min/kg)	T <sub>1/2</sub> (h)	V <sub>ss</sub> (L/kg)	
1982	1996	8.4	3.7	1.5	
(B)					
AUC last (ng h/mL)	AUC/dose (ng h/mL/dose)	C <sub>max</sub> <sup>b</sup> (ng/mL)	T <sub>max</sub> (h)	T <sub>1/2</sub> (h)	F (%)
1764	1774	468	0.5	3.2	89

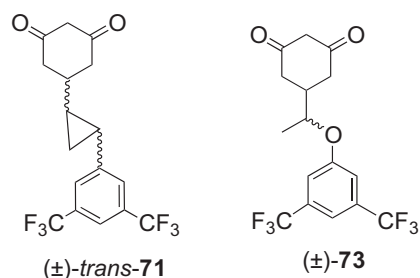
<sup>a</sup> AUC (area under the curve), Cl (clearance), T<sub>1/2</sub> (half life), V<sub>ss</sub> (volume of distribution at steady state).<sup>b</sup> C<sub>max</sub> (maximum concentration), T<sub>max</sub> (time to achieve maximum concentration following dosing), F (bioavailability).**Figure 1.** Kaplan–Meier curve of the effect of **26** on the G93A SOD1 transgenic mouse model for ALS. Untreated: 126.4 ± 4.2; Group 1 (1 mg/kg): 128.9 ± 6.1; Group 2 (10 mg/kg): 130.5 ± 5.8; Group 3 (20 mg/kg): 132.3 ± 4.7.

including cortical neurons. The cortical neuron assay does not produce quantitative results and as a result we can only determine whether a scaffold is active or inactive. The four most promising compounds were **67**, **69**, **71**, and **73**, which have potencies in the cytotoxicity protection assay comparable to that of **26**; however, **69** was inactive in the cortical neuron assay and **67** is not chiral, and we thought that one enantiomer of **71** or **73** would have greater potency and would be more promising to pursue than **67**. Compound **73** also has acceptable mouse ( $t_{1/2}$  45 min) and human ( $t_{1/2}$  71 min) microsomal stability, good plasma stability ( $t_{1/2}$  >60 min), and an excellent efflux ratio (0.1; A→B, 24.8 cm<sup>-6</sup>/s; B→A, 3.1 cm<sup>-6</sup>/s).

**Table 4**Activity of **26** on different cell types

Compound	ALS mouse activity	PC12	SY5Y	HeLa	HEK293	Primary cortical neurons
	+ <sup>a</sup>	+	+	+	+	+
	+ <sup>b</sup>	+	+	+	+	+
<b>26</b> 	–	+	–	–	–	–

The compounds in the first two rows were found earlier to be active in the G93A ALS mouse model.

<sup>a</sup> Refs. 5 and 12.<sup>b</sup> Ref. 6 and unpublished observations.

### 3. Summary

More than 120 CHD analogs have been synthesized, and the structural modification of this scaffold led to the discovery of a more potent analogue (**26**) with an EC<sub>50</sub> of 700 nM. Although the CHD scaffold showed promise for the potential treatment of ALS on the basis of its in vitro efficacy and pharmacokinetic properties, **26** showed very poor activity on a variety of cells, including primary cortical neurons, which may account for its inability to extend the life in the ALS mouse model. Modification of the core structure, however, led to two structures (**71** and **73**) with good potency and the ability to cross into neurons. These compounds are being investigated further.

### 4. Experimental section

#### 4.1. General methods

All reagents were purchased from Aldrich, Alfa Aesar, Oakwood Inc., or Maybridge Ltd and were used without further purification, unless stated otherwise. Tetrahydrofuran was distilled under nitro-

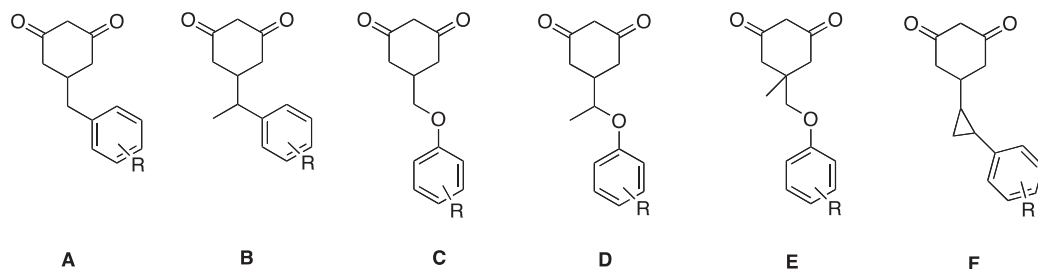


Figure 2. Modified CHD scaffolds.

Table 5  
New synthetic CHD analogs in the PC12-G93A-YFP cell-based assay

CHD	EC <sub>50</sub> <sup>a</sup> (μM)	CHD	EC <sub>50</sub> (μM)	CHD	EC <sub>50</sub>
	1.82		0.90		5.85
	3.43		>32		0.70
	6.28		0.70		2.65
	0.70		1.41		0.70

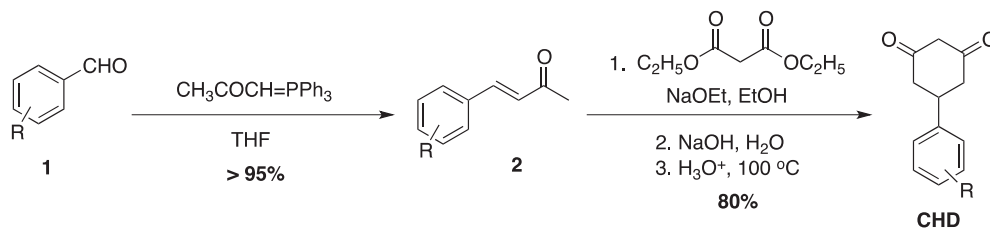
<sup>a</sup> An analog was considered to be inactive when EC<sub>50</sub> >32 μM.

gen from sodium/benzophenone. Thin-layer chromatography was carried out on E. Merck precoated Silica Gel 60 F<sub>254</sub> plates. Compounds were visualized with ferric chloride reagent or a UV lamp. Column chromatography was performed with E. Merck Silica Gel 60 (230–400 mesh). Proton nuclear magnetic resonances (<sup>1</sup>H NMR) were recorded in deuterated solvents on a Varian Inova 400 (400 MHz), a Varian Inova 500 (500 MHz), or a Bruker Ag500 (500 MHz) spectrometer. Chemical shifts are reported in parts per million (ppm, δ) using various solvents as internal standards (CDCl<sub>3</sub>, δ 7.26 ppm; DMSO-*d*<sub>6</sub>, δ 2.50 ppm). <sup>1</sup>H NMR splitting patterns are designated as singlet (s), doublet (d), triplet (t), or quartet (q). Splitting patterns that could not be interpreted or easily visualized were recorded as multiplet (m) or broad (br). Coupling constants are re-

ported in Hertz (Hz). Proton-decoupled carbon (<sup>13</sup>C NMR) spectra were recorded on a Varian Inova 500, a Varian Inova 400, or a Bruker Ag500 (125.7, 100.6, and 125.7 MHz, respectively) spectrometer and are reported in ppm using various solvents as internal standards (CDCl<sub>3</sub>, δ 77.23 ppm; DMSO-*d*<sub>6</sub>, δ 39.52 ppm). High-resolution mass spectra were recorded using a VG70-250SE mass spectrometer.

#### 4.2. General procedure to prepare cyclohexane 1,3-dione (CHD) analogs<sup>7</sup>

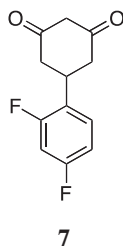
All aldehydes were previously prepared or purchased. Aldehyde **1** (5.0 mmol) was dissolved in THF (20 mL), and 1-(triphenylphos-



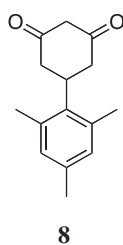
phoranylidene)-2-propanone (1.60 g, 5.0 mmol) was added. The mixture was allowed to stir at room temperature for 12 h. Solvent was removed under vacuum, and the residue was purified by flash column chromatography to provide **2**, which was used directly in the next step, in almost quantitative yield.

Compound **2** (2.0 mmol) and diethyl malonate (2.0 mmol) were dissolved in EtOH (5 mL), and a NaOEt solution (21 wt % in ethanol; 1.50 mL, 4.0 mmol) was added. After being stirred for 12 h, 3 N aq NaOH (20 mL) was added, and stirring was continued for another 12 h. Aqueous 3 N HCl was added until the solution turned cloudy. Ether was used to extract the cloudy mixture until the aqueous layer was clear. The combined organic portions were combined and allowed to stir for 4 h until decarboxylation was complete. Heating might be required in some cases when decarboxylation was not complete at room temperature. The solvent was evaporated, and the crude product was then purified by recrystallization or flash chromatography. The CHD product was typically a white solid, obtained in about an 80% yield, and had an  $R_f = 0.6$  (dichloromethane/methanol = 8:1).

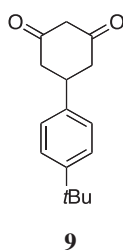
### 4.3. Selected analog characterization



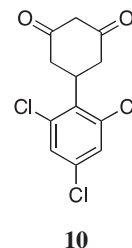
Compound **7** was purified by recrystallization (ether/hexanes) and obtained as a white solid.  $^1\text{H}$  NMR (500 MHz, DMSO- $d_6$ ,  $\delta$ ): 11.30 (br s, 1H), 7.51–7.46 (m, 1H), 7.25–7.20 (m, 1H), 7.11–7.07 (m, 1H), 5.31 (s, 1H), 3.57–3.52 (m, 1H), 2.65–2.60 (m, 2H), 2.42–2.38 (m, 2H);  $^{13}\text{C}$  NMR (125 MHz, DMSO- $d_6$ ,  $\delta$ ): 161.99, 161.89, 161.02, 160.93, 160.04, 159.94, 159.05, 158.96, 129.40, 129.35, 129.32, 129.28, 126.23, 126.20, 126.11, 126.08, 111.57, 111.54, 111.40, 111.38, 104.07, 103.87, 103.65, 103.41, 31.67.



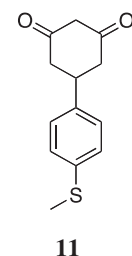
Compound **8** was purified by recrystallization (ether/hexanes) and obtained as a white solid.  $^1\text{H}$  NMR (500 MHz, DMSO- $d_6$ ,  $\delta$ ): 11.21 (br s, 1H), 6.82 (s, 2H), 5.29 (s, 1H), 3.73–3.65 (m, 1H), 2.88–2.83 (m, 2H), 2.32 (s, 3H), 2.17 (s, 6H), 2.16–2.12 (m, 2H);  $^{13}\text{C}$  NMR (125 MHz, DMSO- $d_6$ ,  $\delta$ ): 135.93, 135.21, 135.04, 103.47, 34.09, 21.38, 20.21.



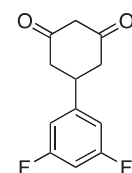
Compound **9** was purified by recrystallization (ether/hexanes) and obtained as a white solid.  $^1\text{H}$  NMR (500 MHz, DMSO- $d_6$ ,  $\delta$ ): 11.17 (br s, 1H), 7.33–7.31 (m, 2H), 7.25–7.23 (m, 2H), 5.28 (s, 1H), 3.26–3.22 (m, 1H), 2.57–2.52 (m, 2H), 2.41–2.37 (m, 2H), 1.27 (s, 9H);  $^{13}\text{C}$  NMR (125 MHz, DMSO- $d_6$ ,  $\delta$ ): 148.79, 140.47, 126.52, 125.16, 103.22, 38.22, 34.08, 30.97.



Compound **10** was purified by recrystallization (ether/hexanes) and obtained as a white solid.  $^1\text{H}$  NMR (500 MHz, DMSO- $d_6$ ,  $\delta$ ): 11.31 (br s, 1H), 7.73 (s, 2H), 5.31 (s, 1H), 4.19–4.15 (m, 1H), 3.24–3.20 (m, 2H), 2.24–2.20 (m, 2H);  $^{13}\text{C}$  NMR (125 MHz, DMSO- $d_6$ ,  $\delta$ ): 134.99, 132.71, 130.17, 128.68, 103.40, 35.07.



Compound **11** was purified by recrystallization (ether/hexanes) and obtained as a white solid.  $^1\text{H}$  NMR (500 MHz, DMSO- $d_6$ ,  $\delta$ ): 11.22 (br s, 1H), 7.29 (d,  $J = 8$  Hz, 2H), 7.22 (d,  $J = 8$  Hz, 2H), 5.28 (s, 1H), 3.30–3.24 (m, 1H), 2.59–2.53 (m, 2H), 2.45 (s, 3H), 2.39–2.36 (m, 2H);  $^{13}\text{C}$  NMR (125 MHz, DMSO- $d_6$ ,  $\delta$ ): 140.35, 136.07, 127.62, 126.26, 103.56, 38.24, 14.91.

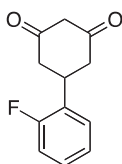


Compound **12** was purified by recrystallization (ether/hexanes) and obtained as a white solid.  $^1\text{H}$  NMR (500 MHz, DMSO- $d_6$ ,  $\delta$ ): 11.30 (br s, 1H), 7.14 (d,  $J = 6.5$  Hz, 2H), 7.10–7.06 (m, 1H), 5.28 (s, 1H), 3.38–3.34 (m, 1H), 2.63–2.58 (m, 2H), 2.40–2.73 (m, 2H);  $^{13}\text{C}$  NMR (125 MHz, DMSO- $d_6$ ,  $\delta$ ): 163.40, 163.29, 161.45, 161.34, 148.27, 148.20, 148.13, 110.44, 110.40, 110.29, 110.25, 103.42, 102.23, 102.02, 101.82, 38.39.



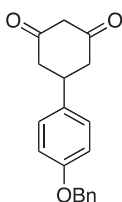
Compound **13** was purified by recrystallization (ether/hexanes) and obtained as a white solid.  $^1\text{H}$  NMR (500 MHz, DMSO- $d_6$ ,  $\delta$ ): 11.34 (br s, 1H), 7.36–7.32 (m, 1H), 7.10–7.07 (m, 2H), 5.30 (s, 1H), 3.65–3.61 (m, 1H), 2.79–2.75 (m, 2H), 2.33–2.30 (m, 2H);  $^{13}\text{C}$  NMR (125 MHz, DMSO- $d_6$ ,  $\delta$ ): 161.78, 161.72, 159.83, 159.76,

129.36, 129.28, 129.19, 117.67, 117.53, 117.39, 112.25, 112.22, 112.08, 112.05, 103.61, 103.37, 103.10, 28.94.



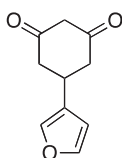
14

Compound **14** was purified by recrystallization (ether/hexanes) and obtained as a white solid.  $^1\text{H}$  NMR (500 MHz,  $\text{DMSO-}d_6$ ,  $\delta$ ): 11.29 (br s, 1H), 7.43–7.41 (m, 1H), 7.32–7.28 (m, 1H), 7.20–7.16 (m, 2H), 5.30 (s, 1H), 3.59–3.53 (m, 1H), 2.65–2.59 (m, 2H), 2.42–2.38 (m, 2H);  $^{13}\text{C}$  NMR (125 MHz,  $\text{DMSO-}d_6$ ,  $\delta$ ): 161.13, 159.19, 129.91, 129.80, 128.65, 128.58, 128.31, 128.27, 124.70, 124.68, 115.56, 115.38, 103.50, 32.16.



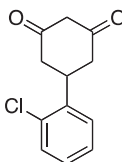
15

Compound **15** was purified by recrystallization (ether/hexanes) and obtained as a white solid.  $^1\text{H}$  NMR (500 MHz,  $\text{DMSO-}d_6$ ,  $\delta$ ): 11.27 (br s, 1H), 7.44–7.43 (m, 2H), 7.40–7.37 (m, 2H), 7.33–7.32 (m, 1H), 7.25 (d,  $J = 8.5$  Hz, 2H), 6.96 (d,  $J = 8.5$  Hz, 2H), 5.30 (s, 1H), 5.07 (s, 2H), 3.26–3.20 (m, 1H), 2.54–2.50 (m, 2H), 2.37–2.34 (m, 2H);  $^{13}\text{C}$  NMR (125 MHz,  $\text{DMSO-}d_6$ ,  $\delta$ ): 157.05, 137.25, 135.86, 128.49, 127.98, 127.84, 127.69, 114.74, 103.57, 69.17, 38.04.



16

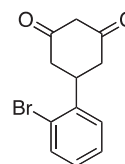
Compound **16** was purified by recrystallization (ether/hexanes) and obtained as a white solid.  $^1\text{H}$  NMR (500 MHz,  $\text{DMSO-}d_6$ ,  $\delta$ ): 11.22 (br s, 1H), 7.58 (s, 1H), 7.50 (s, 1H), 6.52 (s, 1H), 5.25 (s, 1H), 3.38–3.33 (m, 1H), 3.21–3.16 (m, 2H), 2.50–2.45 (m, 2H);  $^{13}\text{C}$  NMR (125 MHz,  $\text{DMSO-}d_6$ ,  $\delta$ ): 143.25, 138.47, 127.51, 109.47, 103.45, 29.47.



17

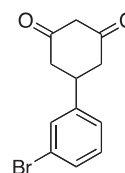
Compound **17** was purified by recrystallization (ether/hexanes) and obtained as a white solid.  $^1\text{H}$  NMR (500 MHz,  $\text{DMSO-}d_6$ ,  $\delta$ ): 11.37 (br s, 1H), 7.51 (d,  $J = 7.5$  Hz, 1H), 7.46 (d,  $J = 8.0$  Hz, 1H), 7.37–7.34 (m, 1H), 7.30–7.27 (m, 1H), 5.31 (s, 1H), 3.71–3.64 (m, 1H), 2.65–2.60 (m, 2H), 2.42–2.39 (m, 2H);  $^{13}\text{C}$  NMR (125 MHz,

$\text{DMSO-}d_6$ ,  $\delta$ ): 140.11, 132.60, 129.62, 128.47, 128.00, 127.71, 103.44, 35.50.



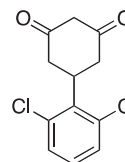
18

Compound **18** was purified by recrystallization (ether/hexanes) and obtained as a white solid.  $^1\text{H}$  NMR (500 MHz,  $\text{DMSO-}d_6$ ,  $\delta$ ): 11.35 (br s, 1H), 7.63 (d,  $J = 8.0$  Hz, 1H), 7.51 (d,  $J = 7.5$  Hz, 1H), 7.41–7.38 (m, 1H), 7.22–7.18 (m, 1H), 5.31 (s, 1H), 3.66–3.60 (m, 1H), 2.65–2.59 (m, 2H), 2.42–2.39 (m, 2H);  $^{13}\text{C}$  NMR (125 MHz,  $\text{DMSO-}d_6$ ,  $\delta$ ): 141.66, 132.94, 128.84, 128.30, 128.10, 123.66, 103.44, 38.24.



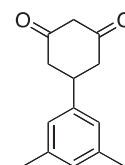
19

Compound **19** was purified by recrystallization (ether/hexanes) and obtained as a white solid.  $^1\text{H}$  NMR (500 MHz,  $\text{DMSO-}d_6$ ,  $\delta$ ): 11.26 (br s, 1H), 7.57 (s, 1H), 7.43 (d,  $J = 7.5$  Hz, 1H), 7.37 (d,  $J = 7.5$  Hz, 1H), 7.30–7.27 (m, 1H), 7.22–7.18 (m, 1H), 5.28 (s, 1H), 3.36–3.30 (m, 1H), 2.63–2.57 (m, 2H), 2.40–2.36 (m, 2H);  $^{13}\text{C}$  NMR (125 MHz,  $\text{DMSO-}d_6$ ,  $\delta$ ): 146.47, 130.71, 129.93, 129.58, 126.21, 121.89, 103.56, 38.41.



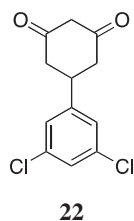
20

Compound **20** was purified by recrystallization (ether/hexanes) and obtained as a white solid.  $^1\text{H}$  NMR (500 MHz,  $\text{DMSO-}d_6$ ,  $\delta$ ): 11.49 (br s, 1H), 7.49 (m, 2H), 7.34–7.30 (m, 1H), 5.32 (s, 1H), 4.22–4.18 (m, 1H), 3.26–3.20 (m, 2H), 2.23–2.20 (m, 2H);  $^{13}\text{C}$  NMR (125 MHz,  $\text{DMSO-}d_6$ ,  $\delta$ ): 135.78, 135.02, 134.37, 130.85, 129.67, 129.22, 103.52, 35.41.

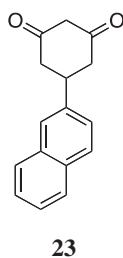


21

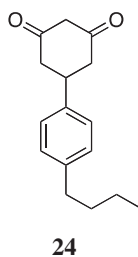
Compound **21** was purified by recrystallization (ether/hexanes) and obtained as a white solid.  $^1\text{H}$  NMR (500 MHz,  $\text{DMSO-}d_6$ ,  $\delta$ ): 11.19 (br s, 1H), 6.92 (s, 2H), 6.84 (s, 1H), 5.28 (s, 1H), 3.21–3.17 (m, 1H), 2.54–2.52 (m, 2H), 2.36–2.33 (m, 2H), 2.23 (s, 6H);  $^{13}\text{C}$  NMR (125 MHz,  $\text{DMSO-}d_6$ ,  $\delta$ ): 143.38, 137.32, 127.97, 124.62, 103.46, 38.66, 30.96. Elemental analysis: Comb. Anal. Calcd for  $\text{C}_{14}\text{H}_{16}\text{O}_2$ : C, 77.75; H, 7.46; O, 14.80. Found: C, 77.55; H, 7.35. Purity: >95%.



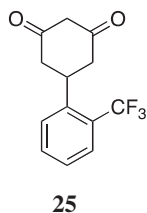
Compound **22** was purified by recrystallization (ether/hexanes) and obtained as a white solid.  $^1\text{H}$  NMR (500 MHz,  $\text{DMSO-}d_6$ ,  $\delta$ ): 11.28 (br s, 1H), 7.46 (s, 3H), 5.28 (s, 1H), 3.39–3.33 (m, 1H), 2.66–2.64 (m, 2H), 2.39–2.36 (m, 2H);  $^{13}\text{C}$  NMR (125 MHz,  $\text{DMSO-}d_6$ ,  $\delta$ ): 147.85, 134.01, 126.30, 126.10, 103.45, 38.21. Elemental analysis: Anal. Calcd for  $\text{C}_{12}\text{H}_{10}\text{Cl}_2\text{O}_2$ : C, 56.06; H, 3.92; Cl, 27.58; O, 12.45. Found: C, 56.13; H, 3.77; Cl, 27.47. Purity: >95%.



Compound **23** was purified by recrystallization (ether/hexanes) and obtained as a white solid.  $^1\text{H}$  NMR (500 MHz,  $\text{DMSO-}d_6$ ,  $\delta$ ): 11.30 (br s, 1H), 7.87–7.83 (m, 3H), 7.79 (s, 1H), 7.57–7.53 (m, 1H), 7.50–7.44 (m, 2H), 5.34 (s, 1H), 3.49–3.44 (m, 1H), 2.73–2.67 (m, 2H), 2.49–2.47 (m, 2H);  $^{13}\text{C}$  NMR (125 MHz,  $\text{DMSO-}d_6$ ,  $\delta$ ): 141.16, 133.11, 132.01, 128.05, 127.64, 127.51, 126.19, 125.82, 125.68, 125.01, 103.64, 38.92.

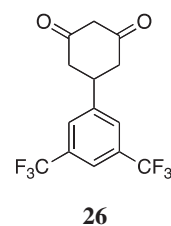


Compound **24** was purified by recrystallization (ether/hexanes) and obtained as a white solid.  $^1\text{H}$  NMR (500 MHz,  $\text{DMSO-}d_6$ ,  $\delta$ ): 11.20 (br s, 1H), 7.24 (d,  $J = 8.0$  Hz, 2H), 7.14 (d,  $J = 8$  Hz, 2H), 5.30 (s, 1H), 3.30–3.26 (m, 1H), 2.60–2.54 (m, 4H), 2.40–2.36 (m, 2H), 1.56–1.51 (m, 2H), 1.30–1.25 (m, 2H), 0.90 (t,  $J = 6.0$  Hz, 3H);  $^{13}\text{C}$  NMR (125 MHz,  $\text{DMSO-}d_6$ ,  $\delta$ ): 140.72, 140.51, 128.31, 126.72, 103.48, 38.36, 34.40, 30.66, 21.90, 13.88.

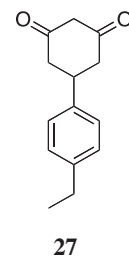


Compound **25** was purified by recrystallization (ether/hexanes) and obtained as a white solid.  $^1\text{H}$  NMR (500 MHz,  $\text{DMSO-}d_6$ ,  $\delta$ ): 11.40 (br s, 1H), 7.90 (d,  $J = 8.0$  Hz, 1H), 7.70–7.68 (m, 2H), 7.48–7.50 (m, 1H), 5.30 (s, 1H), 3.54–3.50 (m, 1H), 2.80–2.76 (m, 2H), 2.30–2.26 (m, 2H);  $^{13}\text{C}$  NMR (125 MHz,  $\text{DMSO-}d_6$ ,  $\delta$ ): 141.98,

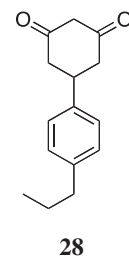
132.94, 128.76, 126.83, 126.60, 126.37, 126.14, 125.75, 125.71, 125.67, 125.62, 125.58, 123.40, 103.20, 35.14.



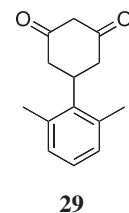
Compound **26** was purified by recrystallization (ether/hexanes) and obtained as a white solid. Mp: 209–211 °C;  $^1\text{H}$  NMR (500 MHz,  $\text{DMSO-}d_6$ ,  $\delta$ ): 11.30 (br s, 1H), 8.12 (s, 2H), 7.95 (s, 1H), 5.31 (s, 1H), 3.62–3.57 (m, 1H), 2.77–2.71 (m, 2H), 2.46–2.43 (m, 2H);  $^{13}\text{C}$  NMR (125 MHz,  $\text{DMSO-}d_6$ ,  $\delta$ ): 146.97, 130.69, 130.43, 130.17, 129.91, 128.23, 126.61, 124.44, 122.27, 120.41, 120.39, 103.46, 38.28. Elemental analysis: Anal. Calcd for  $\text{C}_{14}\text{H}_{10}\text{F}_6\text{O}_2$ : C, 51.86; H, 3.11; F, 35.16; O, 9.87. Found: C, 51.79; H, 3.11; F, 35.31. Purity: >95%.



Compound **27** was purified by recrystallization (ether/hexanes) and obtained as a white solid.  $^1\text{H}$  NMR (500 MHz,  $\text{DMSO-}d_6$ ,  $\delta$ ): 11.23 (br s, 1H), 7.23 (d,  $J = 8.0$  Hz, 2H), 7.15 (d,  $J = 8$  Hz, 2H), 5.31 (s, 1H), 3.28–3.23 (m, 1H), 2.59–2.53 (m, 4H), 2.40–2.36 (m, 2H), 1.16 (t,  $J = 7.5$  Hz, 3H);  $^{13}\text{C}$  NMR (125 MHz,  $\text{DMSO-}d_6$ ,  $\delta$ ): 142.07, 140.86, 127.92, 126.89, 103.62, 38.52, 27.87, 15.75.

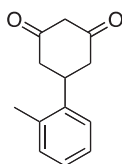


Compound **28** was purified by recrystallization (ether/hexanes) and obtained as a white solid.  $^1\text{H}$  NMR (500 MHz,  $\text{DMSO-}d_6$ ,  $\delta$ ): 11.23 (br s, 1H), 7.24 (d,  $J = 8.0$  Hz, 2H), 7.14 (d,  $J = 8$  Hz, 2H), 5.30 (s, 1H), 3.29–3.24 (m, 1H), 2.60–2.51 (m, 4H), 2.41–2.37 (m, 2H), 1.59–1.54 (m, 2H), 0.90 (t,  $J = 7.5$  Hz, 3H);  $^{13}\text{C}$  NMR (125 MHz,  $\text{DMSO-}d_6$ ,  $\delta$ ): 140.85, 140.43, 128.45, 126.79, 103.58, 38.46, 36.96, 24.22, 13.79.



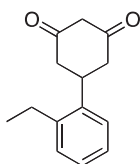
Compound **29** was purified by recrystallization (ether/hexanes) and obtained as a white solid.  $^1\text{H}$  NMR (500 MHz,  $\text{DMSO-}d_6$ ,  $\delta$ ): 11.33 (br s, 1H), 7.03–6.98 (m, 3H), 5.30 (s, 1H), 3.73–3.69 (m, 1H), 2.92–2.86 (m, 2H), 2.35 (s, 6H), 2.22–2.18 (m, 2H);  $^{13}\text{C}$  NMR

(125 MHz, DMSO- $d_6$ ,  $\delta$ ): 138.31, 136.21, 126.39, 103.56, 34.44, 21.51.



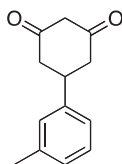
30

Compound **30** was purified by recrystallization (ether/hexanes) and obtained as a white solid.  $^1\text{H}$  NMR (500 MHz, DMSO- $d_6$ ,  $\delta$ ): 11.21 (br s, 1H), 7.36–7.34 (m, 1H), 7.19–7.10 (m, 3H), 5.31 (s, 1H), 3.52–3.46 (m, 1H), 2.60–2.54 (m, 2H), 2.33–2.29 (m, 2H), 2.29 (s, 3H);  $^{13}\text{C}$  NMR (125 MHz, DMSO- $d_6$ ,  $\delta$ ): 141.48, 135.24, 130.40, 126.34, 126.26, 125.69, 103.43, 34.66, 18.95.



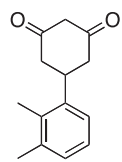
31

Compound **31** was purified by recrystallization (ether/hexanes) and obtained as a white solid.  $^1\text{H}$  NMR (500 MHz, DMSO- $d_6$ ,  $\delta$ ): 11.22 (br s, 1H), 7.41–7.40 (m, 1H), 7.19–7.15 (m, 3H), 5.31 (s, 1H), 3.53–3.47 (m, 1H), 2.65–2.61 (m, 4H), 2.29–2.26 (m, 2H), 1.13 (t,  $J = 7.5$  Hz, 3H);  $^{13}\text{C}$  NMR (125 MHz, DMSO- $d_6$ ,  $\delta$ ): 141.19, 140.93, 128.85, 126.58, 126.23, 126.19, 103.42, 34.16, 25.13, 16.10.



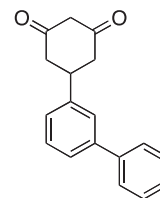
32

Compound **32** was purified by recrystallization (ether/hexanes) and obtained as a white solid.  $^1\text{H}$  NMR (500 MHz, DMSO- $d_6$ ,  $\delta$ ): 11.20 (br s, 1H), 7.21–7.18 (m, 1H), 7.14–7.11 (m, 2H), 7.04–7.03 (m, 1H), 5.28 (s, 1H), 3.27–3.22 (m, 1H), 2.60–2.54 (m, 2H), 2.38–2.35 (m, 2H), 2.28 (s, 3H);  $^{13}\text{C}$  NMR (125 MHz, DMSO- $d_6$ ,  $\delta$ ): 143.53, 137.56, 128.42, 127.66, 127.27, 123.97, 103.55, 38.76, 21.14.



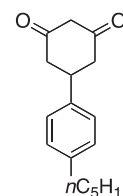
33

Compound **33** was purified by recrystallization (ether/hexanes) and obtained as a white solid.  $^1\text{H}$  NMR (500 MHz, DMSO- $d_6$ ,  $\delta$ ): 11.19 (br s, 1H), 7.17–7.16 (m, 1H), 7.07–7.02 (m, 2H), 5.29 (s, 1H), 3.56 (m, 1H), 2.56–2.50 (m, 2H), 2.33–2.29 (m, 2H), 2.23 (s, 3H), 2.17 (s, 3H);  $^{13}\text{C}$  NMR (125 MHz, DMSO- $d_6$ ,  $\delta$ ): 141.18, 136.54, 133.81, 127.99, 125.54, 123.40, 103.42, 34.87, 20.72, 14.34.



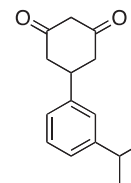
34

Compound **34** was purified by recrystallization (ether/hexanes) and obtained as a white solid.  $^1\text{H}$  NMR (500 MHz, DMSO- $d_6$ ,  $\delta$ ): 11.23 (br s, 1H), 7.70–7.67 (m, 2H), 7.50–7.32 (m, 7H), 5.30 (s, 1H), 3.35–3.33 (m, 1H), 2.70–2.64 (m, 2H), 2.48–2.43 (m, 2H);  $^{13}\text{C}$  NMR (125 MHz, DMSO- $d_6$ ,  $\delta$ ): 144.26, 140.36, 140.18, 129.05, 128.86, 127.41, 126.79, 126.03, 125.49, 124.98, 103.49, 38.82.



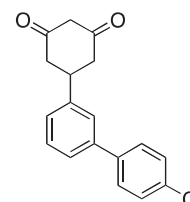
35

Compound **35** was purified by recrystallization (ether/hexanes) and obtained as a white solid.  $^1\text{H}$  NMR (500 MHz, DMSO- $d_6$ ,  $\delta$ ): 11.20 (br s, 1H), 7.24 (d,  $J = 8.0$  Hz, 2H), 7.14 (d,  $J = 8$  Hz, 2H), 5.30 (s, 1H), 3.29–3.23 (m, 1H), 2.60–2.51 (m, 4H), 2.41–2.36 (m, 2H), 1.57–1.52 (m, 2H), 1.33–1.24 (m, 4H), 0.87 (t,  $J = 6.5$  Hz, 3H);  $^{13}\text{C}$  NMR (125 MHz, DMSO- $d_6$ ,  $\delta$ ): 140.79, 140.61, 128.37, 126.78, 103.56, 38.44, 34.78, 31.00, 30.76, 22.02, 13.95.



36

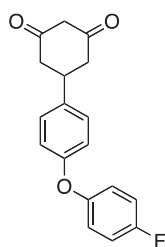
Compound **36** was purified by recrystallization (ether/hexanes) and obtained as a white solid.  $^1\text{H}$  NMR (500 MHz, DMSO- $d_6$ ,  $\delta$ ): 11.20 (br s, 1H), 7.23–7.21 (m, 2H), 7.14–7.09 (m, 2H), 5.28 (s, 1H), 3.29–3.25 (m, 1H), 2.89–2.81 (m, 1H), 2.61–2.56 (m, 2H), 2.39–2.36 (m, 2H), 1.19 (dd,  $J = 7.0$  Hz, 1.0 Hz, 6H);  $^{13}\text{C}$  NMR (125 MHz, DMSO- $d_6$ ,  $\delta$ ): 148.64, 143.55, 128.45, 125.20, 124.50, 124.27, 103.54, 38.89, 33.53, 23.97.



37

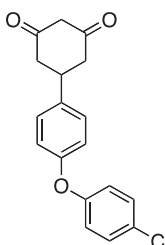
Compound **37** was purified by recrystallization (ether/hexanes) and obtained as a white solid.  $^1\text{H}$  NMR (500 MHz, DMSO- $d_6$ ,  $\delta$ ): 11.25 (br s, 1H), 7.73–7.71 (m, 2H), 7.66 (s, 1H), 7.54–7.51 (m, 3H), 7.43–7.40 (m, 1H), 7.37–7.36 (m, 1H), 5.30 (s, 1H), 3.41 (m, 1H), 2.69 (m, 2H), 2.45–2.43 (m, 2H);  $^{13}\text{C}$  NMR (125 MHz,

DMSO- $d_6$ ,  $\delta$ ): 144.45, 139.04, 139.02, 132.36, 129.23, 128.86, 128.62, 126.49, 125.51, 124.99, 103.55, 38.88.



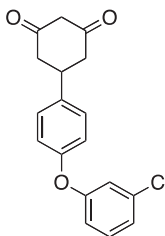
38

Compound **38** was purified by recrystallization (ether/hexanes) and obtained as a white solid.  $^1\text{H}$  NMR (500 MHz, DMSO- $d_6$ ,  $\delta$ ): 11.26 (br s, 1H), 7.35 (d,  $J = 9.0$  Hz, 2H), 7.23–7.21 (m, 2H), 7.06–7.03 (m, 2H), 6.93 (d,  $J = 8.5$  Hz, 2H), 5.30 (s, 1H), 3.33–3.26 (m, 1H), 2.60–2.54 (m, 2H), 2.41–2.37 (m, 2H);  $^{13}\text{C}$  NMR (125 MHz, DMSO- $d_6$ ,  $\delta$ ): 159.18, 157.27, 155.75, 152.74, 152.71, 138.62, 128.58, 120.67, 120.61, 118.15, 116.71, 116.52, 103.59, 38.10.



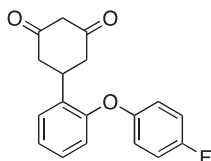
39

Compound **39** was purified by recrystallization (ether/hexanes) and obtained as a white solid.  $^1\text{H}$  NMR (500 MHz, DMSO- $d_6$ ,  $\delta$ ): 11.23 (br s, 1H), 7.42–7.36 (m, 4H), 7.02–6.98 (m, 4H), 5.30 (s, 1H), 3.35–3.29 (m, 1H), 2.61–2.55 (m, 2H), 2.42–2.38 (m, 2H);  $^{13}\text{C}$  NMR (125 MHz, DMSO- $d_6$ ,  $\delta$ ): 155.86, 154.77, 139.21, 129.90, 128.68, 127.06, 120.06, 118.96, 103.58, 38.10.



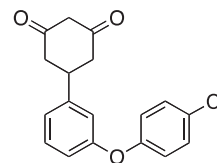
40

Compound **40** was purified by recrystallization (ether/hexanes) and obtained as a white solid.  $^1\text{H}$  NMR (500 MHz, DMSO- $d_6$ ,  $\delta$ ): 11.25 (br s, 1H), 7.39–7.38 (m, 3H), 7.18 (d,  $J = 8.0$  Hz, 2H), 7.02–6.00 (m, 3H), 6.95–6.92 (m, 3H), 5.31 (s, 1H), 3.36–3.29 (m, 1H), 2.62–2.56 (m, 2H), 2.43–2.40 (m, 2H);  $^{13}\text{C}$  NMR (125 MHz, DMSO- $d_6$ ,  $\delta$ ): 158.10, 154.30, 139.57, 134.01, 131.47, 128.75, 123.17, 119.32, 118.10, 116.82, 103.59, 38.12.



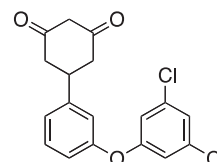
41

Compound **41** was purified by recrystallization (ether/hexanes) and obtained as a white solid.  $^1\text{H}$  NMR (500 MHz, DMSO- $d_6$ ,  $\delta$ ): 11.33 (br s, 1H), 7.50–7.48 (m, 1H), 7.28–7.21 (m, 3H), 7.19–7.16 (m, 1H), 7.02–7.00 (m, 2H), 6.84–6.83 (m, 1H), 5.26 (s, 1H), 3.59–3.56 (m, 1H), 2.69–2.63 (m, 2H), 2.39–2.36 (m, 2H);  $^{13}\text{C}$  NMR (125 MHz, DMSO- $d_6$ ,  $\delta$ ): 158.95, 157.05, 154.14, 153.25, 153.23, 133.90, 128.27, 128.08, 124.18, 119.75, 119.68, 118.75, 116.75, 116.56, 103.37, 32.74.



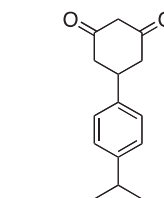
42

Compound **42** was purified by recrystallization (ether/hexanes) and obtained as a white solid.  $^1\text{H}$  NMR (500 MHz, DMSO- $d_6$ ,  $\delta$ ): 11.27 (br s, 1H), 7.43–7.41 (m, 2H), 7.36–7.33 (m, 1H), 7.16–7.15 (m, 1H), 7.08 (s, 1H), 7.03–7.01 (m, 2H), 6.87–6.85 (m, 1H), 5.27 (s, 1H), 3.35–3.29 (m, 1H), 2.62–2.56 (m, 2H), 2.40–2.37 (m, 2H);  $^{13}\text{C}$  NMR (125 MHz, DMSO- $d_6$ ,  $\delta$ ): 156.30, 155.67, 146.16, 130.22, 129.93, 127.12, 122.57, 120.18, 117.73, 116.88, 103.54, 38.57.



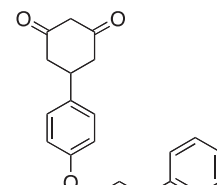
43

Compound **43** was purified by recrystallization (ether/hexanes) and obtained as a white solid.  $^1\text{H}$  NMR (500 MHz, DMSO- $d_6$ ,  $\delta$ ): 11.27 (br s, 1H), 7.41–7.36 (m, 2H), 7.24–7.22 (m, 1H), 7.16 (s, 1H), 7.03 (s, 2H), 6.97–6.95 (m, 1H), 5.27 (s, 1H), 3.35–3.33 (m, 1H), 2.63–2.57 (m, 2H), 2.42–2.38 (m, 2H);  $^{13}\text{C}$  NMR (125 MHz, DMSO- $d_6$ ,  $\delta$ ): 158.69, 155.10, 146.45, 134.96, 130.44, 123.61, 122.88, 118.54, 117.72, 116.95, 103.50, 38.51.



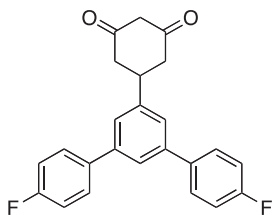
44

Compound **44** was purified by recrystallization (ether/hexanes) and obtained as a white solid.  $^1\text{H}$  NMR (500 MHz, DMSO- $d_6$ ,  $\delta$ ): 11.19 (br s, 1H), 7.25 (d,  $J = 8.5$  Hz, 2H), 7.19 (d,  $J = 8.0$  Hz, 2H), 5.28 (s, 1H), 3.29–3.22 (m, 1H), 2.87–2.82 (m, 1H), 2.59–2.54 (m, 2H), 2.39–2.36 (m, 2H), 1.19 (t,  $J = 7.0$  Hz, 6H);  $^{13}\text{C}$  NMR (125 MHz, DMSO- $d_6$ ,  $\delta$ ): 146.63, 140.96, 126.84, 126.37, 103.54, 38.40, 33.08, 23.95.

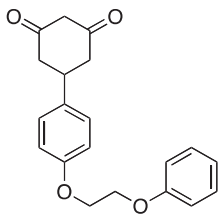


45

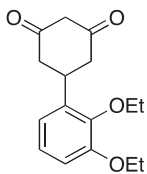
Compound **45** was purified by recrystallization (ether/hexanes) and obtained as a white solid.  $^1\text{H}$  NMR (500 MHz,  $\text{DMSO}-d_6$ ,  $\delta$ ): 11.28 (br s, 1H), 7.30–7.27 (m, 2H), 7.26–7.22 (m, 4H), 7.20–7.17 (m, 1H), 6.88 (d,  $J = 8.5$  Hz, 2H), 5.30 (s, 1H), 3.94 (t,  $J = 6.5$  Hz, 2H), 3.27–3.21 (m, 1H), 2.74 (t,  $J = 7.5$  Hz, 2H), 2.58–2.51 (m, 2H), 2.39–2.35 (m, 2H), 2.03–1.97 (m, 2H);  $^{13}\text{C}$  NMR (125 MHz,  $\text{DMSO}-d_6$ ,  $\delta$ ): 157.33, 141.45, 135.57, 128.40, 127.95, 125.89, 114.41, 103.57, 66.62, 38.03, 31.53, 30.47.

**46**

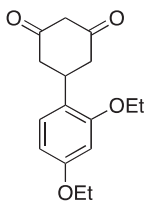
Compound **46** was purified by recrystallization (ether/hexanes) and obtained as a white solid.  $^1\text{H}$  NMR (500 MHz,  $\text{DMSO}-d_6$ ,  $\delta$ ): 11.30 (br s, 1H), 7.86–7.83 (m, 4H), 7.74 (s, 1H), 7.64 (s, 2H), 7.34–7.30 (m, 4H), 5.32 (s, 1H), 3.37 (m, 1H), 2.82–2.76 (m, 2H), 2.51–2.48 (m, 2H);  $^{13}\text{C}$  NMR (125 MHz,  $\text{DMSO}-d_6$ ,  $\delta$ ): 162.96, 161.01, 145.10, 140.04, 136.59, 136.57, 129.11, 129.04, 124.63, 123.46, 115.71, 115.54, 103.45, 38.95.

**47**

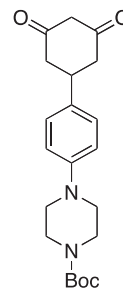
Compound **47** was purified by recrystallization (ether/hexanes) and obtained as a white solid.  $^1\text{H}$  NMR (500 MHz,  $\text{DMSO}-d_6$ ,  $\delta$ ): 11.25 (br s, 1H), 7.32–7.25 (m, 4H), 6.99–6.92 (m, 5H), 5.27 (s, 1H), 4.29 (s, 4H), 3.28–3.23 (m, 1H), 2.58–2.52 (m, 2H), 2.37–2.34 (m, 2H);  $^{13}\text{C}$  NMR (125 MHz,  $\text{DMSO}-d_6$ ,  $\delta$ ): 158.31, 157.01, 135.91, 129.59, 128.01, 120.77, 114.47, 114.46, 103.51, 66.31, 66.18, 38.01.

**48**

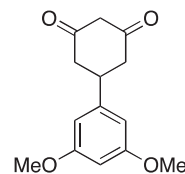
Compound **48** was purified by recrystallization (ether/hexanes) and obtained as a white solid.  $^1\text{H}$  NMR (500 MHz,  $\text{DMSO}-d_6$ ,  $\delta$ ): 11.24 (br s, 1H), 7.00–6.97 (m, 1H), 6.91–6.88 (m, 2H), 5.30 (s, 1H), 4.03–3.94 (m, 4H), 3.66–3.61 (m, 1H), 2.58–2.53 (m, 2H), 2.31–2.29 (m, 2H), 1.35 (t,  $J = 7.0$  Hz, 3H), 1.27 (t,  $J = 7.0$  Hz, 3H);  $^{13}\text{C}$  NMR (125 MHz,  $\text{DMSO}-d_6$ ,  $\delta$ ): 151.61, 145.41, 136.72, 123.84, 118.56, 112.01, 103.46, 68.28, 63.63, 32.49, 15.69, 14.81.

**49**

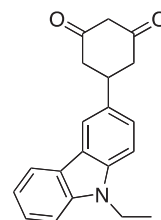
Compound **49** was purified by recrystallization (ether/hexanes) and obtained as a white solid.  $^1\text{H}$  NMR (500 MHz,  $\text{DMSO}-d_6$ ,  $\delta$ ): 11.17 (br s, 1H), 7.11 (d,  $J = 8.5$  Hz, 1H), 6.51 (s, 1H), 6.46 (d,  $J = 8.5$  Hz, 1H), 5.27 (s, 1H), 4.04–3.97 (m, 4H), 3.51–3.45 (m, 1H), 2.58–2.51 (m, 2H), 2.36–2.33 (m, 2H), 1.33–1.29 (m, 6H);  $^{13}\text{C}$  NMR (125 MHz,  $\text{DMSO}-d_6$ ,  $\delta$ ): 158.42, 156.86, 127.43, 123.13, 104.99, 103.41, 99.69, 63.30, 63.02, 32.45, 14.72, 14.70.

**50**

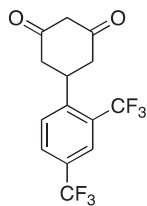
Compound **50** was purified by recrystallization (ether/hexanes) and obtained as a white solid.  $^1\text{H}$  NMR (500 MHz,  $\text{DMSO}-d_6$ ,  $\delta$ ): 11.29 (br s, 1H), 7.19 (d,  $J = 8.5$  Hz, 1H), 6.91 (d,  $J = 8.5$  Hz, 1H), 5.26 (s, 1H), 3.44–3.39 (m, 4H), 3.20 (m, 1H), 3.05–3.03 (m, 4H), 2.55–2.50 (m, 2H), 2.36–2.33 (m, 2H), 1.41 (s, 9H);  $^{13}\text{C}$  NMR (125 MHz,  $\text{DMSO}-d_6$ ,  $\delta$ ): 153.83, 149.65, 134.53, 127.40, 116.15, 103.49, 78.96, 48.80, 37.94, 28.04.

**51**

Compound **51** was purified by recrystallization (ether/hexanes) and obtained as a white solid.  $^1\text{H}$  NMR (500 MHz,  $\text{DMSO}-d_6$ ,  $\delta$ ): 11.20 (br s, 1H), 6.51 (s, 2H), 6.36 (s, 1H), 5.28 (s, 1H), 3.71 (s, 6H), 3.25–3.20 (m, 1H), 2.61–2.57 (m, 2H), 2.38–2.33 (m, 2H);  $^{13}\text{C}$  NMR (125 MHz,  $\text{DMSO}-d_6$ ,  $\delta$ ): 160.45, 145.93, 104.82, 103.41, 98.42, 55.05, 39.03.

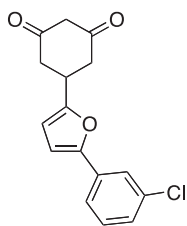
**52**

Compound **52** was purified by recrystallization (ether/hexanes) and obtained as a white solid.  $^1\text{H}$  NMR (500 MHz,  $\text{DMSO}-d_6$ ,  $\delta$ ): 11.29 (br s, 1H), 8.13–8.11 (m, 2H), 7.58–7.52 (m, 2H), 7.45–7.42 (m, 2H), 7.19–7.16 (m, 1H), 5.34 (s, 1H), 4.43 (q,  $J = 7.0$  Hz, 2H), 3.49–3.42 (m, 1H), 2.76–2.70 (m, 2H), 2.50–2.47 (m, 2H), 1.30 (t,  $J = 7.0$  Hz, 3H);  $^{13}\text{C}$  NMR (125 MHz,  $\text{DMSO}-d_6$ ,  $\delta$ ): 139.84, 138.51, 134.12, 125.69, 124.97, 122.22, 122.13, 120.33, 118.62, 118.43, 109.10, 109.08, 103.60, 39.08, 36.97, 13.76.



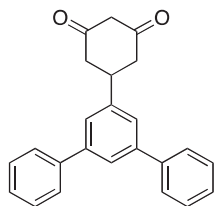
53

Compound **53** was purified by recrystallization (ether/hexanes) and obtained as a white solid.  $^1\text{H}$  NMR (500 MHz,  $\text{DMSO-}d_6$ ,  $\delta$ ): 11.44 (br s, 1H), 8.18 (d,  $J = 8.5$  Hz, 1H), 8.10 (d,  $J = 8.5$  Hz, 1H), 7.98 (s, 1H), 5.33 (s, 1H), 3.62–3.57 (m, 1H), 2.86–2.81 (m, 2H), 2.31–2.27 (m, 2H);  $^{13}\text{C}$  NMR (125 MHz,  $\text{DMSO-}d_6$ ,  $\delta$ ): 146.82, 130.45, 129.80, 129.78, 128.31, 128.05, 127.92, 127.78, 127.68, 127.52, 127.45, 127.21, 126.83, 126.57, 124.65, 124.40, 122.72, 122.47, 122.24, 120.28, 120.07, 103.23, 35.30.



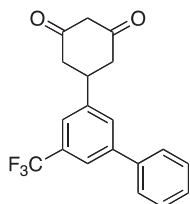
54

Compound **54** was purified by recrystallization (ether/hexanes) and obtained as a white solid.  $^1\text{H}$  NMR (500 MHz,  $\text{DMSO-}d_6$ ,  $\delta$ ): 11.29 (br s, 1H), 7.72 (s, 1H), 7.63 (d,  $J = 8.5$  Hz, 1H), 7.44–7.40 (m, 1H), 7.31 (d,  $J = 8.0$  Hz, 1H), 6.99 (d,  $J = 8.5$  Hz, 1H), 6.31 (d,  $J = 3.5$  Hz, 1H), 5.27 (s, 1H), 3.53–3.49 (m, 1H), 2.67–2.58 (m, 4H);  $^{13}\text{C}$  NMR (125 MHz,  $\text{DMSO-}d_6$ ,  $\delta$ ): 157.18, 150.16, 133.79, 132.32, 130.81, 126.88, 122.67, 121.69, 108.07, 107.38, 103.69, 32.25.



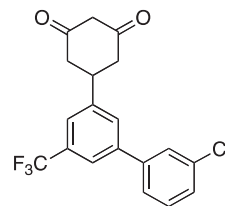
55

Compound **55** was purified by recrystallization (ether/hexanes) and obtained as a white solid.  $^1\text{H}$  NMR (500 MHz,  $\text{DMSO-}d_6$ ,  $\delta$ ): 11.30 (br s, 1H), 7.80–7.78 (m, 4H), 7.65 (s, 2H), 7.46–7.44 (m, 4H), 7.41–7.39 (m, 3H), 5.31 (s, 1H), 3.50–3.45 (m, 1H), 2.80–2.75 (m, 2H), 2.51–2.48 (m, 2H);  $^{13}\text{C}$  NMR (125 MHz,  $\text{DMSO-}d_6$ ,  $\delta$ ): 145.00, 141.08, 140.19, 128.65, 127.55, 127.04, 124.70, 123.53, 103.47, 38.95.



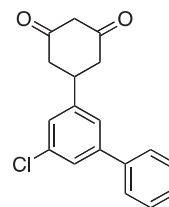
56

Compound **56** was purified by recrystallization (ether/hexanes) and obtained as a white solid.  $^1\text{H}$  NMR (500 MHz,  $\text{DMSO-}d_6$ ,  $\delta$ ): 11.29 (br s, 1H), 7.99 (s, 1H), 7.83 (s, 1H), 7.78–7.76 (m, 2H), 7.73 (s, 1H), 7.52–7.49 (m, 2H), 7.44–7.41 (m, 1H), 5.31 (s, 1H), 3.56–3.50 (m, 1H), 2.79–2.74 (m, 2H), 2.50–2.45 (m, 2H);  $^{13}\text{C}$  NMR (125 MHz,  $\text{DMSO-}d_6$ ,  $\delta$ ): 145.92, 141.53, 138.66, 130.14, 129.88, 129.74, 129.64, 129.10, 128.30, 127.17, 125.35, 123.19, 122.86, 122.83, 122.81, 122.78, 121.58, 121.55, 121.51, 103.53, 38.67.



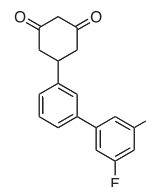
57

Compound **57** was purified by recrystallization (ether/hexanes) and obtained as a white solid.  $^1\text{H}$  NMR (500 MHz,  $\text{DMSO-}d_6$ ,  $\delta$ ): 11.32 (br s, 1H), 8.06 (s, 1H), 7.91–7.90 (m, 2H), 7.77–7.76 (m, 2H), 7.54–7.47 (m, 2H), 5.32 (s, 1H), 3.55–3.50 (m, 1H), 2.82–2.77 (m, 2H), 2.48–2.44 (m, 2H);  $^{13}\text{C}$  NMR (125 MHz,  $\text{DMSO-}d_6$ ,  $\delta$ ): 146.03, 140.73, 139.91, 133.94, 130.87, 130.47, 130.22, 129.97, 129.93, 129.72, 128.13, 127.44, 126.98, 125.90, 125.28, 123.50, 123.47, 123.11, 121.86, 121.83, 120.94, 103.52, 38.69.



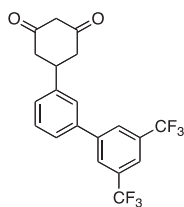
58

Compound **58** was purified by recrystallization (ether/hexanes) and obtained as a white solid.  $^1\text{H}$  NMR (500 MHz,  $\text{DMSO-}d_6$ ,  $\delta$ ): 11.31 (br s, 1H), 7.72–7.70 (m, 1H), 7.64 (s, 1H), 7.58 (s, 1H), 7.49–7.44 (m, 3H), 7.41–7.38 (m, 2H), 5.31 (s, 1H), 3.44–3.37 (m, 1H), 2.74–2.68 (m, 2H), 2.50–2.43 (m, 2H);  $^{13}\text{C}$  NMR (125 MHz,  $\text{DMSO-}d_6$ ,  $\delta$ ): 146.70, 142.44, 138.72, 133.81, 129.04, 128.16, 127.02, 125.98, 124.75, 124.47, 103.56, 38.66.

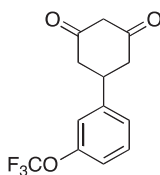


59

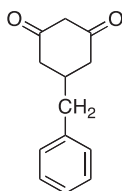
Compound **59** was purified by recrystallization (ether/hexanes) and obtained as a white solid.  $^1\text{H}$  NMR (500 MHz,  $\text{DMSO-}d_6$ ,  $\delta$ ): 11.27 (br s, 1H), 7.75 (s, 1H), 7.61–7.60 (m, 1H), 7.49–7.47 (m, 2H), 7.44–7.39 (m, 2H), 7.23–7.19 (m, 1H), 5.32 (s, 1H), 3.43–3.35 (m, 1H), 2.74–2.68 (m, 2H), 2.46–2.43 (m, 2H);  $^{13}\text{C}$  NMR (125 MHz,  $\text{DMSO-}d_6$ ,  $\delta$ ): 163.94, 163.84, 161.99, 161.89, 144.57, 143.93, 143.85, 143.77, 137.81, 137.79, 137.77, 129.28, 127.44, 125.77, 125.22, 110.02, 109.98, 109.87, 109.82, 103.56, 102.94, 102.74, 102.53, 38.94.

**60**

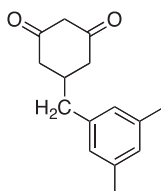
Compound **60** was purified by recrystallization (ether/hexanes) and obtained as a white solid.  $^1\text{H}$  NMR (500 MHz,  $\text{DMSO-}d_6$ ,  $\delta$ ): 11.24 (br s, 1H), 8.38 (s, 2H), 8.09 (s, 1H), 7.91 (s, 1H), 7.74–7.73 (m, 1H), 7.50–7.45 (m, 2H), 5.32 (s, 1H), 3.46–3.40 (m, 1H), 2.80–2.64 (m, 2H), 2.46–2.36 (m, 2H);  $^{13}\text{C}$  NMR (125 MHz,  $\text{DMSO-}d_6$ ,  $\delta$ ): 144.78, 142.75, 137.15, 131.29, 131.03, 130.77, 130.51, 129.41, 127.73, 127.59, 126.69, 126.28, 125.72, 124.52, 123.14, 122.35, 120.95, 120.91, 120.88, 120.18, 105.85, 103.50.

**61**

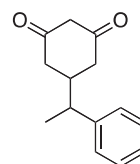
Compound **61** was purified by recrystallization (ether/hexanes) and obtained as a white solid.  $^1\text{H}$  NMR (500 MHz,  $\text{DMSO-}d_6$ ,  $\delta$ ): 11.34 (br s, 1H), 7.65–7.63 (m, 2H), 7.42–7.35 (m, 3H), 5.31 (s, 1H), 3.60–3.54 (m, 1H), 2.69–2.64 (m, 2H), 2.33–2.30 (m, 2H);  $^{13}\text{C}$  NMR (125 MHz,  $\text{DMSO-}d_6$ ,  $\delta$ ): 146.02, 135.55, 128.62, 128.57, 127.93, 123.23, 121.19, 120.88, 119.15, 117.11, 103.42, 32.18.

**62**

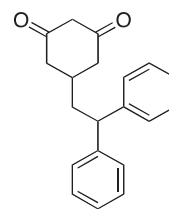
Compound **62** was purified by recrystallization (ether/hexanes) and obtained as a white solid.  $^1\text{H}$  NMR (500 MHz,  $\text{DMSO-}d_6$ ,  $\delta$ ): 11.14 (br s, 1H), 7.31–7.29 (m, 2H), 7.22–7.17 (m, 3H), 5.18 (s, 1H), 2.63 (d,  $J = 7.0$  Hz, 2H), 2.25–2.23 (m, 1H), 2.18–2.10 (m, 4H);  $^{13}\text{C}$  NMR (125 MHz,  $\text{DMSO-}d_6$ ,  $\delta$ ): 139.54, 129.03, 128.35, 126.13, 103.59, 40.80, 35.22.

**63**

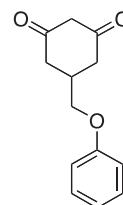
Compound **63** was purified by recrystallization (ether/hexanes) and obtained as a white solid.  $^1\text{H}$  NMR (500 MHz,  $\text{DMSO-}d_6$ ,  $\delta$ ): 11.02 (br s, 1H), 6.83 (s, 1H), 6.78 (s, 2H), 5.18 (s, 1H), 2.54 (d,  $J = 7.0$  Hz, 2H), 2.23 (s, 6H), 2.21–2.08 (m, 5H);  $^{13}\text{C}$  NMR (125 MHz,  $\text{DMSO-}d_6$ ,  $\delta$ ): 139.33, 137.19, 127.55, 126.78, 103.59, 40.73, 35.20, 20.96.

**64**

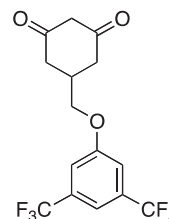
Compound **64** was purified by recrystallization (ether/hexanes) and obtained as a white solid.  $^1\text{H}$  NMR (500 MHz,  $\text{DMSO-}d_6$ ,  $\delta$ ): 11.03 (br s, 1H), 7.32–7.29 (m, 2H), 7.22–7.19 (m, 3H), 5.16 (s, 1H), 2.64–2.58 (m, 1H), 2.41–2.38 (m, 1H), 2.16–2.08 (m, 2H), 1.96–1.91 (m, 1H), 1.82–1.79 (m, 1H), 1.22 (d,  $J = 7.0$  Hz, 3H);  $^{13}\text{C}$  NMR (125 MHz,  $\text{DMSO-}d_6$ ,  $\delta$ ): 145.33, 128.42, 127.41, 126.24, 103.38, 43.80, 39.56, 18.79.

**65**

Compound **65** was purified by recrystallization (ether/hexanes) and obtained as a white solid.  $^1\text{H}$  NMR (500 MHz,  $\text{DMSO-}d_6$ ,  $\delta$ ): 11.06 (br s, 1H), 7.36–7.35 (m, 4H), 7.29–7.26 (m, 4H), 7.18–7.14 (m, 2H), 5.13 (s, 1H), 4.11 (t,  $J = 8.0$  Hz, 1H), 2.28 (m, 2H), 2.12–2.09 (m, 4H), 1.77–1.74 (m, 1H);  $^{13}\text{C}$  NMR (125 MHz,  $\text{DMSO-}d_6$ ,  $\delta$ ): 144.80, 128.51, 127.61, 126.17, 103.46, 99.57, 47.32, 40.19, 31.36.

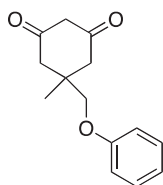
**66**

Compound **66** was purified by recrystallization (ether/hexanes) and obtained as a white solid.  $^1\text{H}$  NMR (500 MHz,  $\text{DMSO-}d_6$ ,  $\delta$ ): 11.19 (br s, 1H), 7.30–7.26 (m, 2H), 6.95–6.91 (m, 3H), 5.24 (s, 1H), 3.93 (d,  $J = 6.0$  Hz, 2H), 2.52–2.46 (m, 1H), 2.41–2.38 (m, 2H), 2.28–2.23 (m, 2H);  $^{13}\text{C}$  NMR (125 MHz,  $\text{DMSO-}d_6$ ,  $\delta$ ): 158.45, 129.56, 120.70, 114.50, 103.66, 70.12, 33.25.

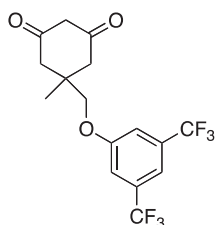
**67**

Compound **67** was purified by recrystallization (ether/hexanes) and obtained as a white solid.  $^1\text{H}$  NMR (500 MHz,  $\text{DMSO-}d_6$ ,  $\delta$ ): 11.25 (br s, 1H), 7.62–7.60 (m, 3H), 5.25 (s, 1H), 4.14 (d,  $J = 6.5$  Hz, 2H), 2.55–2.51 (m, 1H), 2.42–2.38 (m, 2H);  $^{13}\text{C}$  NMR (125 MHz,  $\text{DMSO-}d_6$ ,  $\delta$ ): 159.53, 159.46, 132.01, 131.75, 131.49,

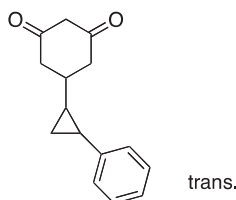
131.23, 126.46, 124.29, 122.12, 119.94, 115.66, 115.63, 113.83, 113.81, 113.77, 103.68, 71.45, 33.09.

**68**

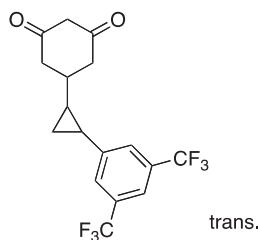
Compound **68** was purified by recrystallization (ether/hexanes) and obtained as a white solid.  $^1\text{H}$  NMR (500 MHz, DMSO- $d_6$ ,  $\delta$ ): 11.15 (br s, 1H), 7.29–7.26 (m, 2H), 6.94–6.92 (m, 3H), 5.23 (s, 1H), 3.77 (s, 2H), 2.50–2.45 (m, 2H), 2.17–2.14 (m, 2H), 1.09 (s, 3H);  $^{13}\text{C}$  NMR (125 MHz, DMSO- $d_6$ ,  $\delta$ ): 158.70, 129.52, 120.73, 114.55, 102.61, 74.13, 36.10, 22.71.

**69**

Compound **69** was purified by recrystallization (ether/hexanes) and obtained as a white solid.  $^1\text{H}$  NMR (500 MHz, DMSO- $d_6$ ,  $\delta$ ): 11.20 (br s, 1H), 7.64 (s, 2H), 7.62 (s, 1H), 5.24 (s, 1H), 3.98 (s, 2H), 2.50 (m, 2H), 2.19–2.15 (m, 2H), 1.10 (s, 3H);  $^{13}\text{C}$  NMR (125 MHz, DMSO- $d_6$ ,  $\delta$ ) 159.68, 159.65, 131.97, 131.71, 131.45, 131.19, 126.45, 124.28, 122.10, 119.94, 115.73, 115.63, 113.86, 113.83, 113.79, 102.67, 75.30, 36.06, 22.51.

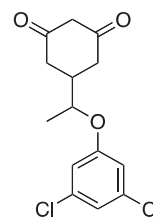
**70**

Compound **70** was purified by recrystallization (ether/hexanes) and obtained as a white solid.  $^1\text{H}$  NMR (500 MHz, DMSO- $d_6$ ,  $\delta$ ): 11.09 (br s, 1H), 7.79 (s, 1H), 7.76 (s, 2H), 5.20 (s, 1H), 3.77 (s, 2H), 2.38–2.34 (m, 2H), 2.26–2.21 (m, 2H), 1.81–1.77 (m, 1H), 1.55–1.49 (m, 1H), 1.03–0.98 (m, 1H), 0.90–0.87 (m, 2H);  $^{13}\text{C}$  NMR (125 MHz, DMSO- $d_6$ ,  $\delta$ ): 143.22, 128.25, 125.55, 125.27, 103.65, 38.25, 28.21, 21.31, 14.23.

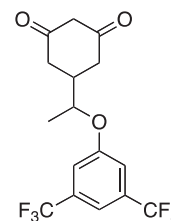
**71**

Compound ( $\pm$ )-**71** was purified by recrystallization (ether/hexanes) and obtained as a white solid. Mp: 154–156 °C;  $^1\text{H}$  NMR

(500 MHz, DMSO- $d_6$ ,  $\delta$ ): 11.09 (br s, 1H), 7.24–7.21 (m, 2H), 7.12–7.09 (m, 1H), 7.06–7.05 (m, 2H), 5.19 (s, 1H), 3.77 (s, 2H), 2.39–2.26 (m, 4H), 2.15–2.11 (m, 1H), 1.60–1.54 (m, 1H), 1.26–1.21 (m, 1H), 1.18–1.14 (m, 1H), 1.10–1.05 (m, 1H);  $^{13}\text{C}$  NMR (125 MHz, DMSO- $d_6$ ,  $\delta$ ): 147.37, 130.61, 130.35, 130.09, 129.83, 126.73, 126.19, 126.16, 124.55, 122.39, 120.22, 118.75, 118.72, 118.69, 118.65, 103.69, 38.13, 29.66, 20.91, 15.29.

**72**

Compound **72** was purified by flash column chromatography (ethyl acetate) and obtained as a white solid.  $^1\text{H}$  NMR (500 MHz, DMSO- $d_6$ ,  $\delta$ ): 11.17 (br s, 1H), 7.13 (s, 1H), 7.07 (s, 1H), 5.22 (s, 1H), 4.54–4.52 (m, 1H), 2.40–2.37 (m, 1H), 2.28–2.24 (m, 4H), 1.22 (d,  $J$  = 6.0 Hz, 3H);  $^{13}\text{C}$  NMR (125 MHz, DMSO- $d_6$ ,  $\delta$ ): 159.15, 134.66, 120.29, 114.76, 103.49, 76.17, 38.46, 16.26.

**73**

Compound ( $\pm$ )-**73** was purified by flash column chromatography (ethyl acetate) and obtained as a white solid. Mp: 137–138 °C;  $^1\text{H}$  NMR (500 MHz, DMSO- $d_6$ ,  $\delta$ ): 11.17 (br s, 1H), 7.62 (s, 2H), 7.60 (s, 1H), 5.22 (s, 1H), 4.75–4.73 (m, 1H), 2.43–2.41 (m, 1H), 2.34–2.28 (m, 4H), 1.25 (d,  $J$  = 6.0 Hz, 3H);  $^{13}\text{C}$  NMR (125 MHz, DMSO- $d_6$ ,  $\delta$ ): 158.65, 132.04, 131.78, 131.52, 131.26, 126.36, 124.19, 122.02, 119.85, 116.38, 113.62, 103.50, 76.31, 38.53, 16.08. Elemental analysis: Anal. Calcd for  $\text{C}_{16}\text{H}_{14}\text{F}_6\text{O}_3$ : C, 52.18; H, 3.83; F, 30.95. Found: C, 52.28; H, 3.70; F, 30.69. Purity: >95%.

#### 4.4. In vitro pharmacokinetic studies

Studies were performed at Apredica, Inc. (Watertown, MA).

#### 4.5. Chromatography and mass spectrometry

Samples were analyzed by LC-MS/MS using an Agilent 6410 mass spectrometer coupled with an Agilent 1200 HPLC and a CTC PAL chilled auto sampler, all controlled by MassHunter software (Agilent). After separation on a C18 reverse phase HPLC column (Agilent, Waters, or equivalent) using a 4 min acetonitrile–water gradient system, peaks were analyzed by mass spectrometry (MS) using ESI ionization in the MRM mode. The mass spectrometer gas flows and voltages were individually tuned to provide optimal signal for each compound. Trial spectra were obtained to determine the best conditions for data collection. The transition(s) that gave the best signal/noise ratio were used for data analysis. See Supplementary data for representative MS spectra and chromatography data.

#### 4.6. Microsomal stability

Test compounds were incubated in duplicate at 5  $\mu\text{M}$  concentration with human or mouse microsomes at 37  $^{\circ}\text{C}$ . The reaction mixture contained 0.275 mg/mL microsomal protein in 100 mM potassium phosphate, 2 mM NADPH, 3 mM  $\text{MgCl}_2$ , pH 7.4. A control was run for each compound omitting NADPH to detect NADPH-independent degradation. After 15 s, 10 min, 20 min, 40 min, and 60 min incubation, aliquots were removed from each experimental and control reaction and mixed with an equal volume of ice-cold Stop Solution (0.3% acetic acid in acetonitrile containing 0.3  $\mu\text{M}$  haloperidol as an internal standard). Stopped reactions were incubated at least 10 min at  $-20^{\circ}\text{C}$ , and an additional volume of water was added. The samples were centrifuged to remove precipitated protein, and the supernatants were analyzed by LC–MS/MS to quantify the remaining parent molecule. Excel was used for the calculations. The Response Ratio (RR) was calculated using Mass Hunter software by dividing the peak area of the analyte by the peak area of the internal standard. The relative ratio was calculated by dividing the RR with NADPH by the RR from the  $-$ NADPH control at the same time point.

$$(\text{Relative Ratio} = \text{PA}_{+\text{NADPH}}/\text{PA}_{-\text{NADPH}})$$

The % compound remaining (RE) was calculated by dividing the relative ratio of the sample in question by  $A_0$ ,

$$\text{RE} = \text{RR}/A_0$$

where  $A_0$  is a correction factor for small differences in the starting concentration and extraction efficiency. Curve fitting was used to determine  $A_0$ ,  $k$  (first-order rate constant) using an exponential fit with  $1/Y$  weighing. The half-life was calculated as:  $T_{1/2} = \ln(2)/k$ . The intrinsic clearance was calculated as follows:  $\text{CL}_{\text{int}} = (0.693/T_{1/2}) \times (\text{mL incubation/mg microsomal protein}) \times (\text{mg microsomal protein/g liver}) \times (\text{g liver/kg bodyweight})$ . The scale-up factor for microsomes protein to g of liver is 45 mg/g of liver. Liver weights used for human and mice were 20 g/kg body weight and 34 g/kg body weight, respectively. The units on the  $\text{CL}_{\text{int}}$  are mL/min/kg. See Supplementary data for human/mouse microsomal stability results with CMB-086874.

#### 4.7. Caco-2 monolayer permeability

Caco-2 permeability is measured by detecting the amount of compound that permeates through a confluent monolayer of Caco-2 cells. Caco-2 cells grown in tissue culture flasks were trypsinized, suspended in medium, and the suspensions were applied to wells of a collagen-coated BioCoat Cell Environment in a 24-well format (BD Biosciences). The cells were allowed to grow and differentiate for three weeks, feeding at 2-day intervals.

Stock solutions of 10 mM test compound or control prepared in DMSO were used to prepare solutions for the Caco-2 permeability studies. For apical to basolateral (A $\rightarrow$ B), the apical (A-side) buffer contained 50  $\mu\text{M}$  test compound or control and 100  $\mu\text{M}$  Lucifer yellow dye in the transport buffer (1.98 g/L glucose in 10 mM HEPES, 1  $\times$  Hank's Balanced Slat Solution) at pH 6.5; the basolateral (B-side) buffer was the transport buffer at pH 7.4. For B $\rightarrow$ A studies, the A-side buffer contained 100  $\mu\text{M}$  Lucifer yellow in the transport buffer, pH 6.5, and the B-side buffer contained 50  $\mu\text{M}$  test compound or control in the transport buffer, pH 7.4. The Caco-2 cells were incubated with these buffers for 2 h, and the cell buffers and dosing solutions were removed for analysis.

To verify that the Caco-2 cell monolayer was properly formed, an aliquot of the cell buffer from each well was analyzed by fluorescence to determine the transport of the impermeable Lucifer Yellow dye. In all cases, acceptable transport of Lucifer Yellow was observed (<1% transport in 2 h).

Caco-2 results are reported as apparent permeability,  $P_{\text{app}}$ , expressed in units of  $10^{-6}$  cm/s:  $P_{\text{app}} = \frac{dQ/dt}{c_0 A}$  where  $dQ/dt$  is the rate of permeation (mol test compound transported per unit time),  $c_0$  is the initial concentration of test compound, and  $A$  is the area of the cell monolayer. See Supplementary data for Caco-2 permeability of CMB-086874.

#### 4.8. Solubility screen

The solubility of the test compounds in PBS was estimated by absorbance. Threefold serial dilutions were prepared in DMSO at 100 times the final concentration. This DMSO stock was diluted to the final concentration in PBS, the plate was incubated at room temperature for 1 h, then it was examined visually for the formation of precipitate, and the absorbance at 450 nm was measured. For non-colored compounds the absorbance value was used to detect solubility, while for highly colored compounds, visual inspection was used. The highest concentration that was not visibly cloudy and whose absorbance was not different from background was judged to be the solubility limit (see Supplementary data).

#### 4.9. Stability in plasma and PBS

The test compounds, with warfarin and diltiazem as controls, were incubated in mouse plasma and PBS in duplicate at 5  $\mu\text{M}$  concentration. The time-zero samples were taken immediately (15 s) after adding the compounds. The plate containing the plasma and PBS samples was incubated at 37  $^{\circ}\text{C}$ , and then time points were taken at 10, 20, 40, and 60 min in the same way. The plasma samples and PBS samples were precipitated with acetonitrile containing haloperidol as an internal standard and either centrifuged or filtered through a Varian Captiva plate (following the manufacturer's directions) to remove precipitated protein. The samples were then analyzed by LC–MS/MS.

The response ratio (RR = area of analyte peak divided by the area of the internal standard peak), as calculated by the LC–MS software, was used for determining the plasma stability. The relative ratio was calculated by dividing the RR from plasma by the RR from the PBS control at the same time point.

$$(\text{Relative Ratio} = \text{RR}_{\text{plasma}}/\text{RR}_{\text{PBS}})$$

The % compound remaining (RE) was calculated as described above for microsomes. To determine PBS half-life, the RR was fit to a first-order exponential curve to determine  $A_{\text{PBS}}$  and  $k_{\text{PBS}}$ :  $\text{RR} = A_{\text{PBS}}e^{-k_{\text{PBS}}t}$ . The half-life was calculated as above:  $T_{1/2} = \ln(2)/k_{\text{PBS}}$ . See Supplementary data for mouse plasma stability of CMB-086874.

#### 4.10. Primary cortical neuron assay

Primary rat cortical tissue was purchased from Neuromics Inc., Edina, MN and used to initiate primary cortical neuron cultures. The tissue was isolated from micro-surgically dissected E18 embryonic Sprague/Dawley or Fischer 344 rat brain and shipped in a nutrient rich medium under refrigeration.

To isolate neurons, the tissue was incubated with papain at a concentration of 2 mg/mL in Hibernate without calcium for 30 min at 37  $^{\circ}\text{C}$ . The enzymatic solution was then removed, and 1 mL of culture media (Neurobasal, B27, 0.5 mM glutamine) was added. A sterile Pasteur pipette was used to gently disperse the cells, which were then washed, re-suspended and counted. The cells were plated on poly-D-lysine coated 96-well plates at a density of 20,000 cells/well and incubated at 37  $^{\circ}\text{C}$  in a 5%  $\text{CO}_2$ -humidified atmosphere for 5 days prior to use in compound testing. By microscopic inspection, the resulting cultures consisted of  $\sim$ 90% neurons.

Test compounds were assayed in six-point dose response experiments. The highest compound concentration tested was 100  $\mu$ M, which was then diluted by approximately one-third with each subsequent dose. After 24 h incubation with the compounds, MG132 was added at a final concentration of 100 nM, a dose that produces an approximately 70% loss of viability. Cell viability was measured 48 h later using the fluorescent viability probe, Calcein-AM (Molecular Probes, Invitrogen, Carlesbad, CA). Briefly, cells were washed twice with PBS, Calcein-AM was added at a final concentration of 1  $\mu$ M for 20 min at room temperature, and fluorescence intensity was then read in a POLARstar fluorescence plate reader (BMG). Compounds that restored viability at any dose to a level equal or higher than 5 standard deviations from MG132 controls were considered active.

#### 4.11. Radioligand binding assays

These studies were carried out by MDS Pharma Services.

#### 4.12. Effect of compound 26 on hERG potassium channels

FASTPatch hERG screen assay was carried out by ChanTest Corporation (Cleveland, OH). Cloned hERG potassium channels were expressed in human embryonic kidney cells (HEK293).

#### 4.13. General procedures for in vivo experiments

Male transgenic ALS mice of the G93A H1 high-expressor strain (Jackson Laboratories, Bar Harbor, ME, USA) were bred with females having a similar background (B6/SJLFl). Offspring were genotyped using a PCR assay on tail DNA. To ensure homogeneity of the cohorts tested, we developed a standardized method by which to select mice. Mice were randomized from 24 litters all within 4 days of age from the same 'f' generation removed from the founding mice in our colony. Bodyweights were taken at 20 days, and mice were equally distributed according to weight within each experimental cohort. Mice under 8 g at 20 days were excluded from the experiments. Only male mice were used in the treatment studies because we have observed gender differences in survival in the G93A transgenic ALS mouse model.<sup>9</sup> These experiments were carried out in accordance with the National Institutes of Health (NIH) Guide for the Care and Use of Laboratory Animals, and were approved by both the Veterans Administration and the University Animal Care Committees. Based upon previous studies,<sup>10,11</sup> a dose–response study was performed. Groups ( $n = 10$ ) of wild-type (WT), untreated G93A, and G93A mice received 1, 10, and 20 mg/kg of **26** injected intraperitoneally once a day in the morning. Mice were observed twice daily, morning and afternoon, for any adverse events. Compound **26** was dissolved in phosphate-buffered saline (PBS) with 0.1% DMSO, and fresh solutions were prepared daily. Treatment was started at 42 days, as our studies demonstrate that clinical disease onset begins on or about this age. The ALS mice were euthanized when they were unable to right themselves after being placed on their back for 30 s. Some deaths occurred overnight and were recorded the following morning. Two independent observers who were blinded to the treatment assignment agreed when animals should be euthanized. Survival data were analyzed by means of Kaplan–Meier survival curves.

#### 4.14. Plasma concentration and blood brain barrier penetration of 26

Compound **26** was administered in mice as a single bolus intraperitoneal injection of 50 mg/kg. A group of 18 mice were used and blood and brain tissue samples were immediately quenched in liquid nitrogen and stored at  $-80^{\circ}\text{C}$  for analysis. Samples were collected at 0 h (no drug), 1 h, 3 h, 6 h, 12 h, and 24 h.

#### 4.15. Effect of 26 in ALS mouse model

A dose–response curve was implemented with 5 cohorts of mice (littermate wild type untreated mice, untreated mutant SOD 1 G93A mice, and 3 treated cohorts of mutant SOD 1 G93A mice at 1 mg/kg, 10 mg/kg, and 20 mg/kg). Mice were weighed and administered drug daily via intraperitoneal injection at the same time of day. The mice were monitored twice daily for any adverse events and were euthanized at end stage disease using the righting mechanism as a surrogate measure of death.

#### Acknowledgments

We thank the National Institutes of Health [1R43NS057849], the ALS Association (TREAT program), the Department of Defense [AL093052], and the Veterans Administration Pittsburgh Healthcare System, 7180 Highland Drive, Pittsburgh, PA for their generous support of the research project. The authors are grateful to Biogen Idec, Inc. for carrying out the in vivo rat PK profiling tests, in vitro P450 reversible inhibition study, the plasma binding affinity assay, the hERG inhibition assay, and for funding to MDS Pharma Service (now Ricerca Biosciences, LLC), who carried out the LeadProfilingScreen of **26**.

#### References and notes

1. Brujin, L. I.; Miller, T. M.; Cleveland, D. W. *Annu. Rev. Neurosci.* **2004**, *27*, 723.
2. (a) Hirtz, D.; Thurman, D. J.; Gwinn-Hardy, K.; Mohamed, M.; Chaudhuri, A. R.; Zalutsky, R. *Neurology* **2007**, *68*, 326; (b) Cronin, S.; Hardiman, O.; Traynor, B. J. *Neurol.* **2007**, *68*, 1002.
3. (a) Matsumoto, G.; Stojanovic, A.; Holmber, C. I.; Kim, S.; Morimoto, R. I. *J. Cell Biol.* **2005**, *171*, 75; (b) Matsumoto, G.; Kim, S.; Morimoto, R. I. *J. Biol. Chem.* **2006**, *281*, 4477.
4. Benmohamed, R.; Arvanites, A. C.; Kim, J.; Ferrante, R. J.; Silverman, R. B.; Morimoto, R. I.; Kirsch, D. R. *Amyotroph. Lat. Scler.* **2011**, *12*, 87.
5. Chen, T.; Benmohamed, R.; Arvanites, A. C.; Ranaivo, H. R.; Morimoto, R. I.; Ferrante, R. J.; Watterson, D. M.; Kirsch, D. R.; Silverman, R. B. *Bioorg. Med. Chem.* **2011**, *19*, 613.
6. Xia, G.; Benmohamed, R.; Kim, J.; Arvanites, A. C.; Morimoto, R. I.; Ferrante, R. J.; Kirsch, D. R.; Silverman, R. B. *J. Med. Chem.* **2011**, *54*, 2409.
7. Yoshimoto, Y.; Kunimoto, K.; Tada, S.; Tomita, T.; Wada, T.; Seto, E.; Murayama, M.; Shibata, Y.; Nomura, A.; Ohata, K. *J. Med. Chem.* **1977**, *20*, 709.
8. (a) Gurney, M. E.; Pu, H.; Chiu, A. Y.; Dal Canto, M. C.; Polchow, C. Y., et al *Science* **1994**, *264*, 1772; (b) Pitzer, C.; Kruger, C.; Plaas, C.; Kirsch, F.; Dittgen, T., et al *Brain* **2008**, *131*, 3335.
9. Ferrante, R. J.; Klein, A. M.; Beal, M. F. *J. Mol. Neurosci.* **2001**, *17*, 89.
10. Ryu, H.; Smith, K.; Camelo, S. I.; Carreras, I.; Lee, J.; Iglesias, A. H.; Dangond, F.; Cormier, K. A.; Cudkovic, M. E.; Brown, R. H., Jr.; Ferrante, R. J. *J. Neurochem.* **2005**, *93*, 1087.
11. Ryu, H.; Ferrante, R. J. *MRCM* **2007**, *7*, 141.
12. Chen, T.; Benmohamed, R.; Kim, J.; Smith, K.; Amante, D.; Morimoto, R. I.; Kirsch, D. R.; Ferrante, R. J.; Silverman, R. B. *J. Med. Chem.* **2012**, in press.